5124 J. Med. Chem. 2009, 52, 5124–5143
DOI: 10.1021/jm9005803

Journal of Medicinal Chemistry Article

Radiolabeled 5-Iodo-3′-*O*-(17β-succinyl-5α-androstan-3-one)-2′-deoxyuridine and Its 5′-Monophosphate for Imaging and Therapy of Androgen Receptor-Positive Cancers: Synthesis and Biological Evaluation

Zbigniew P. Kortylewicz,* Jessica Nearman, and Janina Baranowska-Kortylewicz*

Department of Radiation Oncology, J. Bruce Henriksen Cancer Research Laboratories, University of Nebraska Medical Center, 986850 Nebraska Medical Center, Omaha, Nebraska 68198-6850

Received May 5, 2009

High levels of androgen receptor (AR) are often indicative of recurrent, advanced, or metastatic cancers. These conditions are also characterized by a high proliferative fraction. 5-Radioiodo-3′-*O*-(17β-succinyl-5α-androstan-3-one)-2′-deoxyuridine **8** and 5-radioiodo-3′-*O*-(17β-succinyl-5α-androstan-3-one)-2′-deoxyuridin-5′-yl monophosphate **13** target AR. They are also degraded intracellularly to 5-radioiodo-2′-deoxyuridine **1** and its monophosphate **20**, respectively, which can participate in the DNA synthesis. Both drugs were prepared at the no-carrier-added level. Precursors and methods are readily adaptable to radiolabeling with various radiohalides suitable for SPECT and PET imaging, as well as endoradiotherapy. In vitro and in vivo studies confirm the AR-dependent interactions. Both drugs bind to sex hormone binding globulin. This binding significantly improves their stability in serum. Biodistribution and imaging studies show preferential uptake and retention of **8** and **13** in ip xenografts of human ovarian adenocarcinoma cells NIH:OVCAR-3, which overexpress AR. When these drugs are administered at therapeutic dose levels, a significant tumor growth arrest is observed.

Introduction

Androgen receptor (AR[a]) is commonly expressed in many cancers.[1−20] AR is the most frequently detected sex hormone receptor in breast cancer cells. Its expression is reported in > 70% of all breast cancer cases[1−4] and in 45−50% of patients with estrogen receptor-negative breast cancer.[4] The AR status, not estrogen or progesterone receptor, is predictive of tumor response to hormonal therapies.[21] AR is expressed in most histological types and stages of prostate cancers including primary, metastatic, and hormone refractory malignant tissues.[5−10] High levels of AR predict shorter time to the biochemical relapse after the androgen deprivation therapy.[8] The amplification of AR is associated with the relapsing disease.[9] The AR signaling pathway is critical to the development and progression of prostate cancer.[10] AR has also been detected in the majority of ovarian cancers;[12−15] however, the AR status does not appear to be a strong prognostic factor in ovarian cancer. No definitive correlations between the presence of AR, blood hormone levels, stage of disease, and tumor histology have been established[22−25] even though the pathophysiology of this disease supports a strong connection with androgens.[26] Studies into the relevance of AR in various cancers are impeded because accurate in situ measurements of the AR expression remain technically challenging.

One feature common to AR-expressing cancers is their high S phase fraction.[27−34] The survival and the time to progression for patients with ovarian cancer are correlated with the tumor S-phase fraction. Patients with high S-phase fraction tumors have significantly lower 5-year survival than patients with low S-phase fraction tumors. Median time to recurrence is 48 and 17 months for low and high S-phase fraction tumor patients, respectively.[28] There is a significant heterogeneity of the mean S-phase fraction between diploid and aneuploid samples depending on the tumor site. Diploid lymph node metastases have the lowest mean S-phase fraction (< 7.2%), and the aneuploid lymph node metastases have the highest mean S-phase fraction (22.3%).[29] In prostate cancer, the S-phase fraction is significantly higher in tumors with high AR density.[30,31] The recurrent prostate tumors, which have the AR amplification, are highly proliferative and are more often aneuploid compared to tumors with no AR amplification.[31] This implies increased AR-mediated cell proliferation in the recurrent tumor cells.

Drugs described in this study take into account these two predominant characteristics of the disease in advanced or recurrent stages and comprise 5α-dihydrotestosterone (DHT) as the AR-based tumor-seeking moiety and 5-radioiodo-2′-deoxyuridine or its phosphate as the S-phase specific agents to preferentially target and kill these cancer cells, which are AR-positive and have a high S-phase fraction. This particular cell population characterizes tumors that are prone to relapse.[29,33,34] When radiolabeled with diagnostic radionuclides, drugs described below will allow for the simultaneous evaluation of the AR status and the S-phase fraction, thereby facilitating tumor staging and planning of the therapy. To date, 11 new drugs were designed, synthesized, and tested. Two drugs, which were identified as good candidates for translational and clinical studies, are described.

*To whom correspondence should be addressed. For Z.P.K.: telephone, 402-559-1030; fax, 402-559-9127; e-mail, zkortylewicz@unmc.edu. For J.B.-K.: telephone, 402-559-8906; fax, 402-559-9127; e-mail, jbaranow@unmc.edu.

[a] Abbreviations: AR, androgen receptor; SHBG, sex hormone binding globulin; DHT, 5α-dihydrotestosterone; HPLC, high-performance liquid chromatography; ITLC, instant thin layer chromatography, FBS, fetal bovine serum; PET, positron emission tomography, SPECT, single photon emission computed tomography; PBS, phosphate buffered saline; ip, intraperitoneal.

 Published on Web 08/04/2009

Scheme 1. Syntheses of Target Compounds **8** and **13**[a]

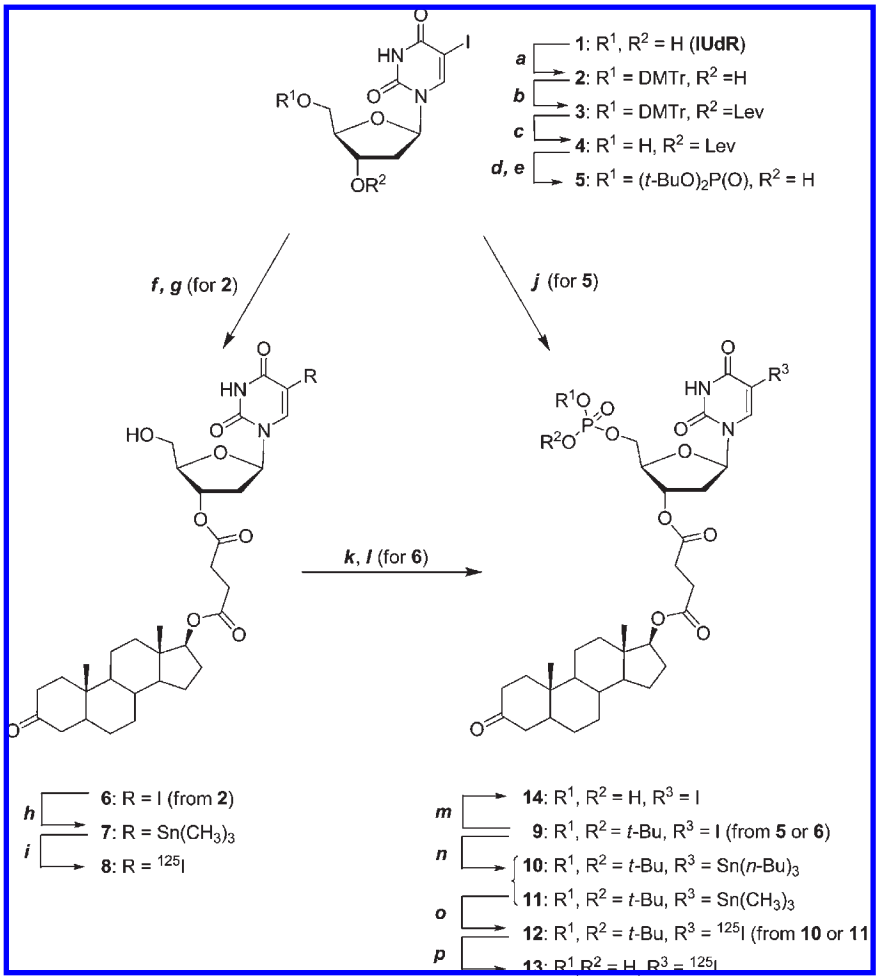

[a] (a) DMTrCl (1.1 equiv), Et_3N (1.2 equiv), DMAP (0.05 equiv), in dry pyridine, 0 °C to room temp, 6 h; (b) 4-oxopentanoic acid, DCC/DMAP in CH_2Cl_2, room temp, 3 h; (c) $ZrCl_4$ (1.1 equiv) in CH_3CN, room temp, 20 min; (d) (i) 1*H* tetrazole (4.5 equiv); (ii) $(t\text{-BuO})_2PN(i\text{-Pr})_2$ (1.2 equiv), 0 °C to room temp, in dry DMF/THF (3:4), ~4 h (TLC monitoring); (iii) *t*-BuOOH, 5−6 M solution in *n*- decane (2.0 equiv), −16 °C to room temp, 1 h; (e) $H_2NNH_2 \cdot H_2O$, pyridine, CH_3COOH, room temp, 2 min; (f) **2**, dihydrotestosterone 17β-succinate, DCC/DMAP in CH_2Cl_2, room temp, or dihydrotestosterone 17β-succinate activated with CDI (1.15 equiv), CH_2Cl_2, 0 °C to room temp, 40 min; (g) $ZrCl_4$ (1.25 equiv) in CH_3CN, room temp, 30 min; (h) $Sn_2(CH_3)_6$ (1.2 equiv), $(Ph_3P)Pd(II)Cl_2$ (0.07 equiv), in dioxane refluxed under N_2, ~3 h (TLC monitoring); (i) (i) $Na^{125}I$/NaOH (1−10 mCi), 30% H_2O_2 (5 μL), TFA/CH_3CN (0.1% v/v), room temp, 15 min; (ii) HPLC purification; (j) **5**, as for step f ; (k) (i) 1*H* tetrazole (5.0 equiv); (ii) $(t\text{-BuO})_2PN(i\text{-Pr})_2$ (1.25 equiv), 4 °C to room temp, dry CH_3CN, overnight (TLC monitoring); (l) *t*-BuOOH, 5−6 M solution in *n*-decane (5.5 equiv), 0 °C to room temp, 1 h; (m) **9** dried sample, TFA/CH_3CN anhydrous, room temp, ~40 min (TLC monitoring). (n) In preparation of **10**: $Sn_2(n\text{- Bu})_6$ (1.25 equiv), $(Ph_3P)Pd(II)Cl_2$ (0.1 equiv), EtOAc refluxed under N_2, 6 h. In preparation of **11**: $Sn_2(CH_3)_6$ (1.5 equiv), $(Ph_3P)Pd(II)Cl_2$ (0.07 equiv), EtOAc refluxed under N_2, 2 h. (o) As for step i; (p) (i) dried sample of **12** (1−10 mCi) under N_2, anhydrous CH_3CN (200 μL), TFA (30 μL), ~60 min (HPLC monitoring); (ii) HPLC purification.

Results

Chemistry. Syntheses of ^{125}I-radioiodinated compounds **8**, **13**, **17**, and **20**, based on the non-carrier-added electrophilic iododestannylation of the corresponding trialkylorganotin precursors,[35,36] are detailed in Schemes 1 and 2. Nonradioactive iodo analogues **5** and **15**, as well as **6** and **9** (those containing the androstan-3-one moiety) required in the preparation of stannanes **7**, **10**, **11**, **16**, and **18**, were constructed first. The esterification of dihydrotestosterone 17β-succinate[37] with **2** and the subsequent deprotection of the 5′-position on uridine led to 5-iodo-3′-*O*-(17β-succinyl-5α-androstan-3-one)-2′-deoxyuridine **6** isolated in 73% overall yield. The phosphorylation of uridine **6** by the reactive phosphoramidite provided the corresponding phosphotriester **9**, however, in only 11% overall yield. This low yield is most likely caused by the large size of dihydrotestosterone at the 3′-position on uridine. As a result, 5-iodo-*O*,*O*′-(di-*tert*-butyl)-2′-deoxyuridin-5′-yl phosphate **5** was synthesized first and was subsequently reacted with dihydrotestosterone 17β-succinate to furnish **9** in satisfactory yield of 69%.

Initially, the starting phosphotriester **5** was prepared by the 5′-O-phosphitylation of 5-iodo-3′-*O*-levulinyl-2′-deoxyuridine **4** with di-*tert*-butyl *N*,*N*-diisopropylphosphoramidite and excess of 1*H*-tetrazole, followed by one-pot oxidation of phosphite with *tert*-butyl hydroperoxide, and the 3′-*O*-Lev group deprotection.[38] With this approach, the average overall yield of **5** was 64%. Later, to simplify this route, the preparation of levulinate **4** was omitted and the direct phosphorylation of unprotected 5-iodo-2′-deoxyuridine (IUdR) **1** was adopted, furnishing a mixture of three products: the desired phosphotriester **5** (5′-regioisomer) in 48% yield, the 3′-isomer (34%), and the 3′,5′-disubstituted

uridine (15%). These were separated on a silica gel column with no difficulties. Both pathways led to phosphate **5** with practically the same efficiencies when yields of required protection/deprotection steps are taken into account.

Organotin precursors **7**, **11**, **16**, and **18** were prepared by the stannylation of iodouridines **5**, **6**, **9**, and **15**, using hexamethylditin, and were carried out in the presence of palladium-(II) catalyst. Phosphotriester **9** was also reacted with hexa-*n*-butylditin, giving the corresponding tri-*n*-butyltin derivative **10**. The tri-*n*-butyltin precursor **10**, having a much higher hydrophobicity than stannane **11**, eluted from the HPLC column 23 min later during the purification of ^{125}I-labeled **12**, which allowed for a fast and more efficient separation of the radiolabeled product, especially when larger volumes, up to 1 mL, of the crude reaction mixture were injected. The remaining ^{125}I-labeled target compounds **8**, **17**, and **19** were sufficiently well resolved from their trimethyltin precursors **7**, **16**, and **18**, allowing the preparation of radioiodinated no-carrier-added products, with high specific activities, using a single HPLC purification.

Exploratory radioiododestannylations were performed with the trimethyltin precursor **7** (120 μg), Na^{125}I (10 μL, 1 mCi), and four different oxidants. Literature procedures were carried out with chloramine T,[39] Iodogen,[40] hydrogen peroxide,[41] and peracetic acid.[42] In all reactions, the product was at least 80−95% **8** with 5−15% of inorganic radioiodide. Co-injections of the radiolabeled material with the independently prepared iodo standard **6** confirmed the identity of radioiodinated **8**.

N-Chloro-substituted oxidants led to the measurable chlorodestannylation of **7** (~11% by HPLC). The proton destannylation, observed to some extent in all reactions, was definitely elevated when peracetic acid was used. Radioiododestannylation performed with hydrogen peroxide as the oxidant consistently gave the best results with an average radiochemical yield of >85%. For the synthesis of uridines **8**, **12**, **17**, and **19**, the standard radioiododestannylation procedure, originally developed for the synthesis of 5-[^{125}I]-iodo-2′-deoxyuridine,[43] was followed.

The *tert*-butyl esters of the (*t*-BuO)$_2$P(O) group in phosphotriesters **12** and **19** were cleaved using a mixture of TFA/CH$_3$CN (10−13%, v/v, 100 μL) in less than 1 h, cleanly producing the corresponding target radioiodinated phosphates **13** and **20** in high radiochemical yield. In both cases, the progress of hydrolysis was monitored using HPLC (see Supporting Information pp S39, S40, S58). However, to achieve the completion of hydrolysis, it was critical to use anhydrous *tert*-butyl phosphotriesters **12** and **19**. In the

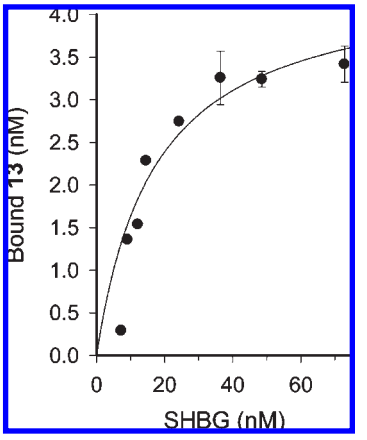

Figure 1. Binding of compound **13** to sex hormone binding globulin. Samples were diluted with PBS, pH 7.1, to achieve indicated above concentrations of SHBG. Compound **13** was dissolved in CH$_3$CN, and 10 μL (on average 5.4 μCi) was added to each SHBG dilution. Resulting mixtures were vortexed and incubated for 30 min at ambient temperature. Aliquots were withdrawn, injected, and analyzed on the size exclusion HPLC column.

Scheme 2. Syntheses of Control Compounds **17** and **20**[a]

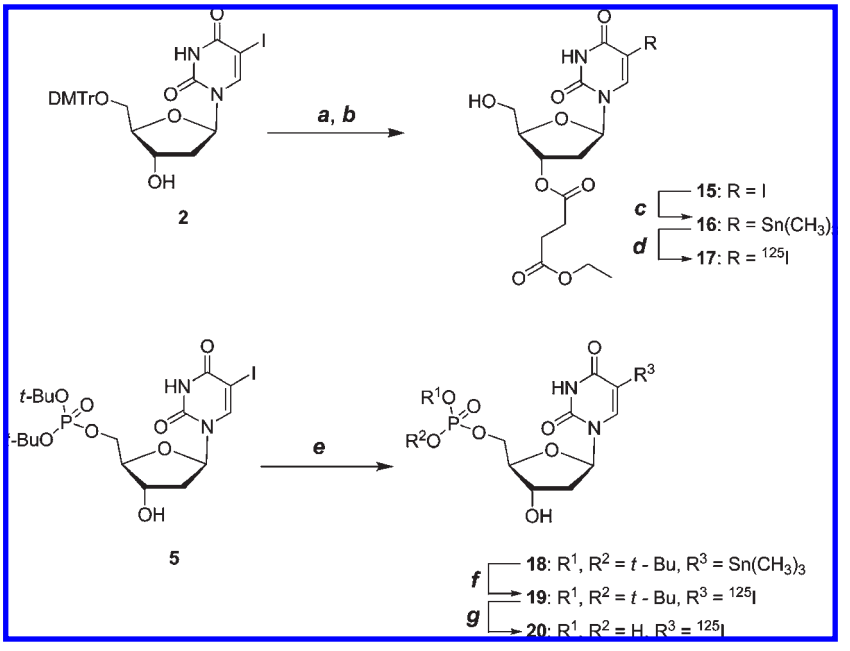

[a] (a) monoethyl succinate (1.25 equiv), DCC/DMAP, CH$_2$Cl$_2$, room temp, 2 h; (b) TFA (90%), *tert*-butanol, room temp, 2 h (TLC monitoring); (c) Sn$_2$(CH$_3$)$_6$ (1.5 equiv), (Ph$_3$P)Pd(II)Cl$_2$ (0.015 equiv), in EtOAc refluxed under N$_2$, 40 min (TLC monitoring); (d) (i) Na^{125}I/NaOH (1−10 mCi), 30% H$_2$O$_2$ (5 μL), TFA/CH$_3$CN (0.1% v/v), room temp, 15 min; (ii) HPLC purification; (e) as for step c, refluxed in dioxane, 3 h; (f) as for step d; (g) (i) dried sample of **19** (1−10 mCi) under N$_2$, anhydrous CH$_3$CN (200 μL), TFA (30 μL), ~40 min (HPLC monitoring); (ii) HPLC purification.

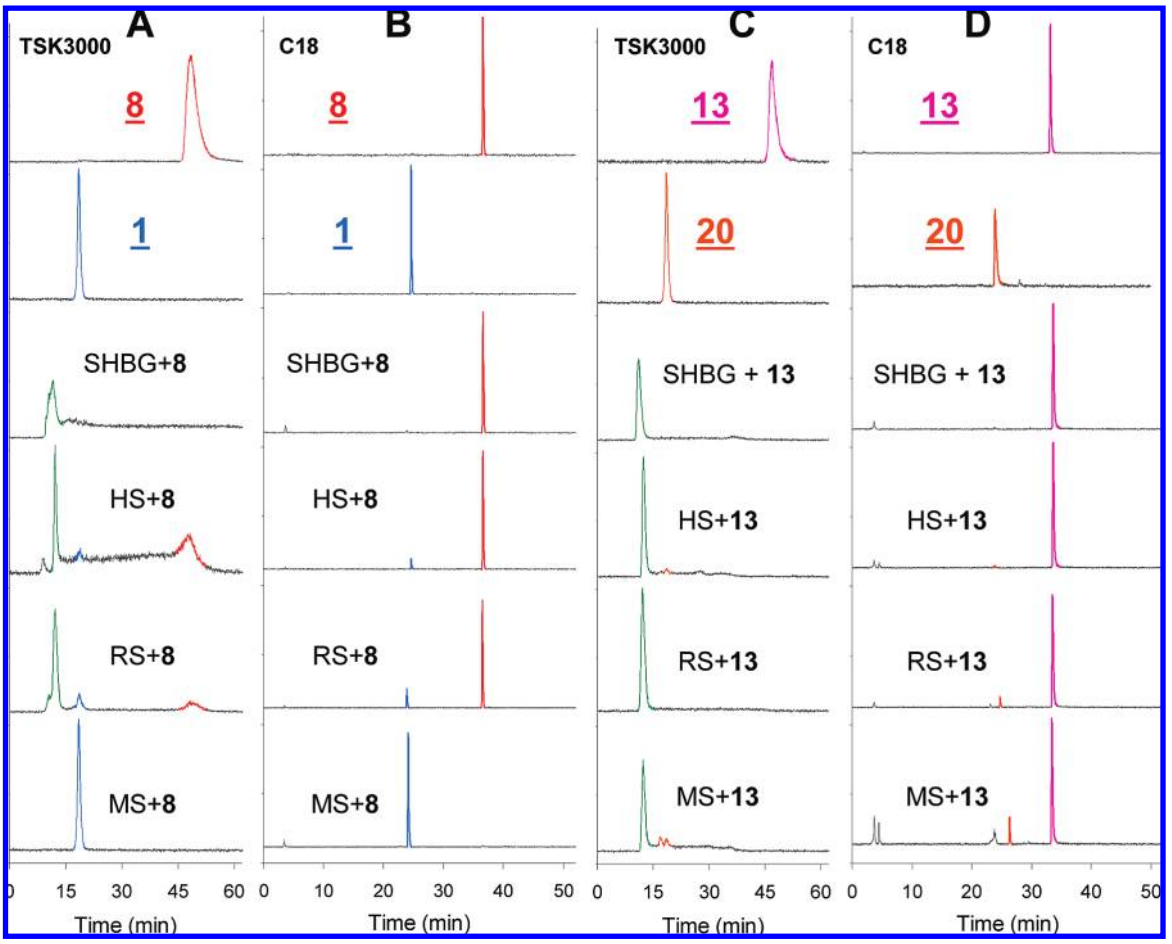

Figure 2. HPLC analyses of **8** and **13** interactions with purified human SHBG and human (HS), rabbit (RS), and mouse (MS) serum. After 60 min of incubation, compounds were analyzed on a size-exclusion column (data for **8** are shown in panel A; data for **13** are shown in panel C). Size exclusion conditions are as follows: solvent A, 0.1 M potassium phosphate buffer and 0.1 M Na_2SO_4, 1:1 (v/v), pH 6.8; solvent B, CH_3CN. Elution parameters on TSK3000 column are as follows: solvent A for 20 min followed by a linear gradient of solvent B from 0% to 40% over 20 min, held at 40% B for 30 min, flow rate 0.7 mL/min. HPLC analyses of extracts were performed on a reverse phase column (panels B and D for **8** and **13**, respectively). Reverse phase conditions are as follows: solvent A, H_2O, and solvent B, CH_3CN, both containing 0.07% TFA. Elution conditions are as follows: 100% solvent A for 10 min, then a linear gradient of solvent B from 0% to 95% over 30 min, held at 95% B for 20 min. Flow rate was 0.8 mL/min. The top row shows size exclusion and C18 HPLC traces of pure **8** (red peak in columns A and B) and pure **13** (purple peak in columns C and D). The second row shows size exclusion and C18 HPLC traces of pure **1** (blue peak in columns A and B), which is the degradation product of **8**, and **20** (orange peak in columns C and D), which is the degradation product of **13**. The green peaks in all panels correspond to **8** and **13** bound to SHBG.

presence of water, the cleavage process always stopped at the (*t*-BuO)(OH)P(O)-phosphate diester stage. In the hydrolysis of dried, anhydrous **12** (10 mCi), three components, the desired $(HO)_2P(O)$-phosphate **13** (92%), (*t*-BuO)(HO)P(O)-phosphate diester (5%), and $(t\text{-BuO})_2P(O)$-triester **12** (≤2%), were consistently formed and separated from the reaction mixture. The cleavage rates of *tert*-butyl ester groups of anhydrous [^{125}I]iodo-2′-deoxyuridine-5′-monophosphate di-*tert*-butyl phosphotriester **19** were faster. Within 35 min of hydrolysis of **19**, 10 mCi used in the form of dried residue, the target [^{125}I]iodo-2′-deoxyuridine-5′-monophosphate **20** (96%) was separated alongside mono-*tert*-butyl ester of **19** (3%). HPLC analyses indicated no less than 95% of the intact radiochemically pure product after 24 h of storage. HPLC co-injections of the independently prepared iodo standards **6**, **9**, **14**, and **15** with the corresponding radioiodinated derivatives **8**, **12**, **13**, and **17** were used to confirm the identity of radiolabeled compounds. HPLC retention times of 5-[^{125}I]iodo-2′-deoxyuridine-5′-monophosphate **20** were identical to the retention time of commercially available 5-iodo-2′-deoxyuridine 5′-monophosphate.

Binding and Stability Studies. Binding of compounds **8**, **13**, **17**, and **20** to human sex hormone binding globulin (SHBG) was measured using size-exclusion HPLC and instant thin layer chromatography (ITLC) methods. Figure 1 shows a typical binding isotherm for **13** derived from the HPLC data. K_d for this compound was estimated at 17.2 ± 4.2 nM and B_{max} at 4.5 ± 0.4 nM. Interactions of all compounds with human, rabbit, and mouse serum were also analyzed. Data for **8** and **13** are shown in Figures 2 and 3. The nonspecific control compounds **17** and **20** are in the Supporting Information (S53, S54, S61, S62). Additionally, to confirm the specific binding to SHBG and the lack of binding to albumin, all radioactive drugs were incubated with albumin alone, PBS, and human SHBG mixed with albumin, and these mixtures were analyzed on the size exclusion column (Supporting Information, pp S25, S44, S45, S48).

Compounds **8** and **13** bind to pure SHBG isolated from human serum. Both compounds also bind to SHBG in rabbit and human serum (Figures 1, 2, and 3). This binding confers a significant degree of stability, as indicated by the presence of intact **8** and **13** in extracts prepared from the incubation

mixtures and analyzed on a C18 column. Compound **8** does not bind to mouse serum (bottom panel in Figure 2A), whereas **13** appears to bind to some unidentified component of mouse serum (bottom panel in Figure 2C).

Adult mice do not have circulating SHBG. When **8**, which does not seem to bind to any component of the mouse serum, is incubated in mouse serum, < 1.5% of intact **8** remains after 10 min of incubation. In contrast, > 84% and > 91% **8** remains intact after 60 min of incubation upon binding to SHBG in rabbit or human serum, respectively. Similar stabilities are also seen for **13** bound to SHBG in rabbit and human serum. The weak binding to some component(s) of mouse serum allows ~60% of **13** to remain intact after 40 min of incubation. Neither the control reagent **17** nor compound **20**, which is the metabolite of **13**, binds to SHBG or to any component of analyzed sera; however, their stability depends on the source of serum. After 60 min of incubation in mouse and rabbit serum, only a trace (< 2%) of **17** remains intact. In contrast, in human serum, > 90% of **17** is still present after 60 min incubation (Supporting Information S53, S54). In rabbit and human serum, ~30% of intact **20** is isolated after 60 min of incubation. Compound **20** does not survive incubation in mouse serum, and after 60 min only **1** is detectable (Supporting Information pp S61, S62).

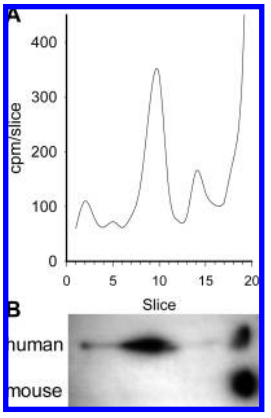

Figure 3. Instant thin layer chromatography analyses of **8** binding to human SHBG and human and mouse serum. (A) Compound **8** was incubated with human SHBG for 60 min. ITLC plate, eluted with 1:9 (v/v) ethanol/PBS mixture, was cut into 5 mm slices, and their radioactive content was determined in a γ counter. (B) Compound **8** was incubated for 60 min with human and mouse serum diluted with PBS at 1:5 (v/v) ratio. The eluted plate was placed on the Kodak XAR imaging film, which was exposed for ~2 h and developed. Spots migrating with the solvent front correspond to the unbound ligand.

The longitudinal stability of **8** and **13** in mouse, human, and rabbit serum was also evaluated. Figure 4 illustrates the time course of **8** degradation in rabbit and human serum. Mouse serum data are shown in the Supporting Information (S30, S31, S46). Half-lives calculated from the monoexponential fit are 5.7 ± 0.6 h and 14.7 ± 1.3 h in rabbit and human serum, respectively (S34 in Supporting Information).

Prior to biological studies, the stability of **8** and **13** was also determined in PBS and RPMI-1640 cell culture medium. Both compounds are stable in PBS. Only after prolonged 24 h of incubation in RPMI-1640 medium is ~30% of **8** hydrolyzed (Supporting Information pp S26−S28). Figure 5A illustrates the time course of **8** breakdown when incubated in

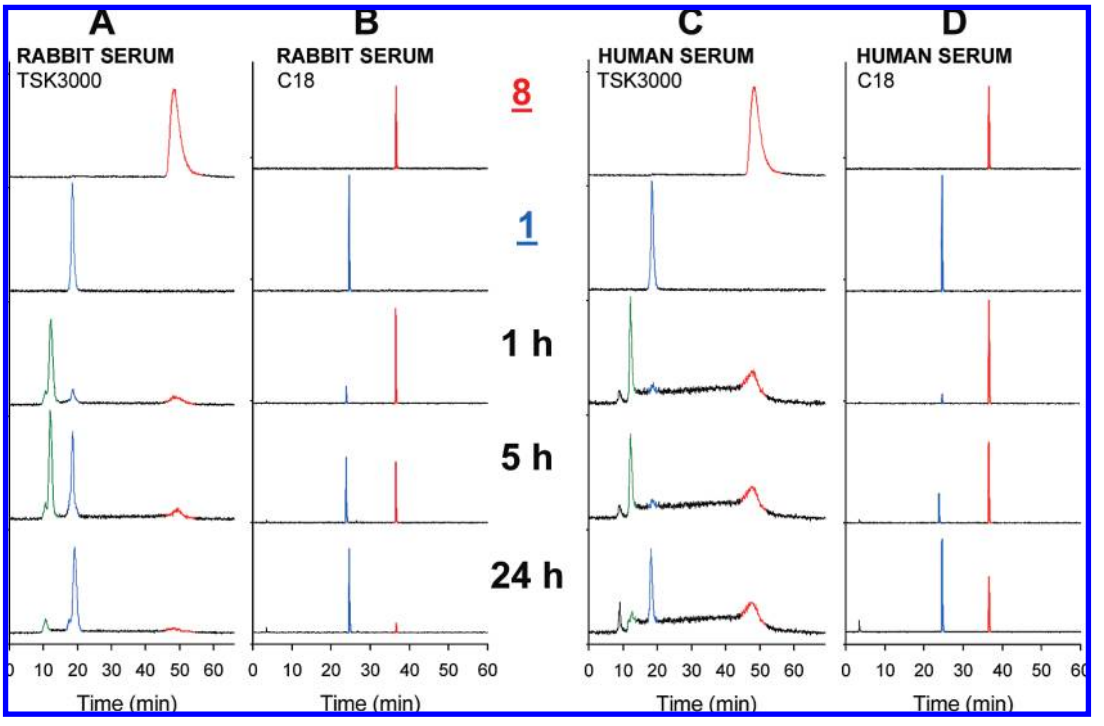

Figure 4. Stability of compound **8** in rabbit serum (panels A and B) and human serum (panels C and D). After indicated incubation times, aliquots of the mixtures were analyzed on a size-exclusion column (panels A and C) under the conditions described in Figure 2. Extracts were analyzed on a reversed phase HPLC column (panels B and D) using conditions described in Figure 2. Top two rows of all panels show size exclusion and C18 HPLC traces of pure **8** (red peak) and **1** (blue peak). Panels labeled 1 h, 5 h, and 24 h are mixtures of **8** with rabbit and human serum incubated at ambient temperature for 1, 5, and 24 h before HPLC analyses. Green peaks designate **8** bound to SHBG in serum. Red peak is the intact **8** present in the incubation mixture. Blue peak corresponds to **1**, a degradation product derived from **8**, present in the incubation mixture.

RPMI-1640 serum-free medium. In a span of 6 h, ~90% of **8** remains intact and the half-life is estimated at 54.2 ± 2.5 h. The stability of **8** is strongly affected by the presence of cancer cells. When similar experiments are conducted in the presence of living OVCAR-3 cells (Figure 5B), ~60% of **8** is degraded within 4 h, releasing **1** and 3′-succinate of **1** into the culture medium.

The half-life of **8** in the presence of cancer cells is estimated at 3.2 ± 0.26 h, indicating rapid intracellular metabolism of **8** to **1**. ^{125}IUdR **1** can participate in DNA synthesis; however, it does not have any features that would permit its retention inside the cell and for this reason, it gradually appears in the cell culture medium.

The studies on the effect of OVCAR-3 cells on the stability of **13** were not conducted because the intracellular retention of 5′-monophosphate **20** confounds the distribution of radioactive components in the cell culture medium.

In Vitro Studies in Cancer Cells. The uptake and subcellular distribution of **8** and **13** were analyzed in four human cancer cell lines characterized by diverse levels of the AR expression. LNCaP and NIH:OVCAR-3 have high and comparable levels of the AR expression when cultured in vitro, in terms of both the AR mRNA level and the expression of AR protein.[44−46] MCF-7 cells have the AR protein expression at the limit of detection,[47,48] while PC-3 cells do not express AR.[45] The degree of **8** and **13** uptake and DNA incorporation reflects this variability in the AR expression.

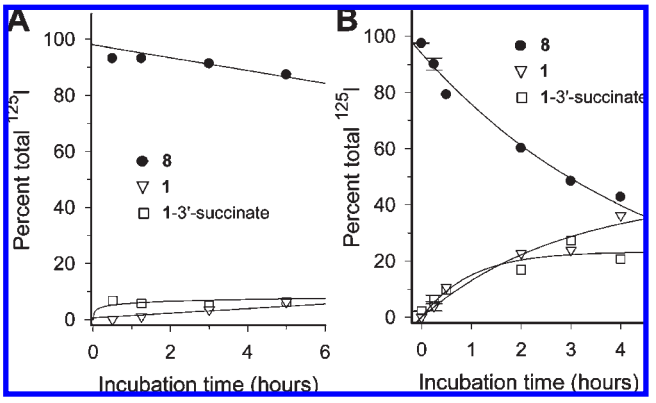

Figure 5. Stability of compound **8**: (A) radioactive product distribution when **8** is incubated in the RPMI-1640 serum-free cell culture medium; (B) examination of breakdown products of **8** in the presence of proliferating NIH:OVCAR-3 human ovarian adenocarcinoma cells grown in the complete RPMI-1640 medium.

Figure 6 illustrates the concentration and time-dependent accumulation of **8** in LNCaP cells. In the presence of living cells, **8** undergoes metabolic intracellular degradation to ^{125}IUdR **1** (Figure 5B), which can participate in the DNA synthesis. For this reason, cell uptake studies were first done in a single-cell suspension of LNCaP cells, i.e., conditions that do not permit cellular proliferation in this cell line (Figure 6A and Figure 6B), and therefore, the uptake of **1** into the DNA is not expected.

During the initial 2 h incubation, there is a time-dependent increase in the cellular accumulation of **8**. After this time, as **8** is being converted into **1**, there is a decline in the retention of radioactivity in a whole cell and in a cell nucleus. This decline roughly parallels the rate of appearance of **1** in the cell culture medium, suggesting that the uptake in the single-cell suspension is dependent on the extracellular concentration of **8**. To verify this observation, nonproliferating LNCaP cells in suspension were exposed to ~10× higher concentration of **8** (Figure 6B), and indeed the cellular retention of radioactivity increased by a factor of ~10.

The uptake of **8** is significantly higher in proliferating LNCaP cells grown as a monolayer because when the internalized **8** is degraded to **1** (^{125}IUdR), an analogue of thymidine, proliferating cells can utilize **1** in the DNA synthesis (Figure 6C). Analyses of data shown in Figure 6C using a single cell-binding isotherm (cpm/cell bound) give an estimated B_{max} of 1.4×10^{-6} pmol/cell, which corresponds to ~850 000 ^{125}I per cell. This level of ^{125}I incorporation into the cancer cell's DNA is lethal.[49−52] Previous studies indicate that the localized energy from ^{125}I disintegrations within DNA in mammalian cells produces approximately one double-strand break and 1.3 single-strand breaks per ^{125}I disintegration.[50] Only about 50% of these breaks are repaired.[51,52]

NIH:OVCAR-3 cells exposed to either **8** or **13** show the uptake and intracellular accumulation of ^{125}I similar to LNCaP cells. The intracellular retention of radioactivity is higher for compound **13** compared to **8** (Figure 7). The key reason for this difference is that metabolite **1**, on release from **8**, is not retained within the cell, whereas monophosphate **20** liberated intracellularly from **13** is trapped inside the cell and is standing by to participate in the DNA synthesis, regardless of the cell cycle phase at which **13** became available for the

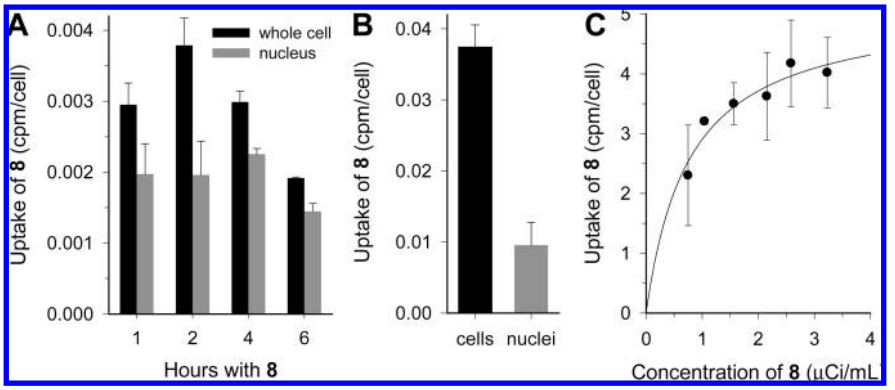

Figure 6. Uptake and subcellular distribution of **8** in human prostate cancer LNCaP cells (low passage), which express high levels of AR. (A) Whole cell and nuclear uptake as a function of the exposure time to the radioactive drug **8**. Living but not proliferating cells were maintained as a cell suspension in RPMI-1640 medium containing **8** at a concentration of 0.03 μCi/mL. (B) The same experiment conducted at the concentration of **8** at 0.37 μCi/mL. (C) Concentration dependent uptake of **8** in proliferating LNCaP cells grown as a monolayer after 24 h of exposure to **8**.

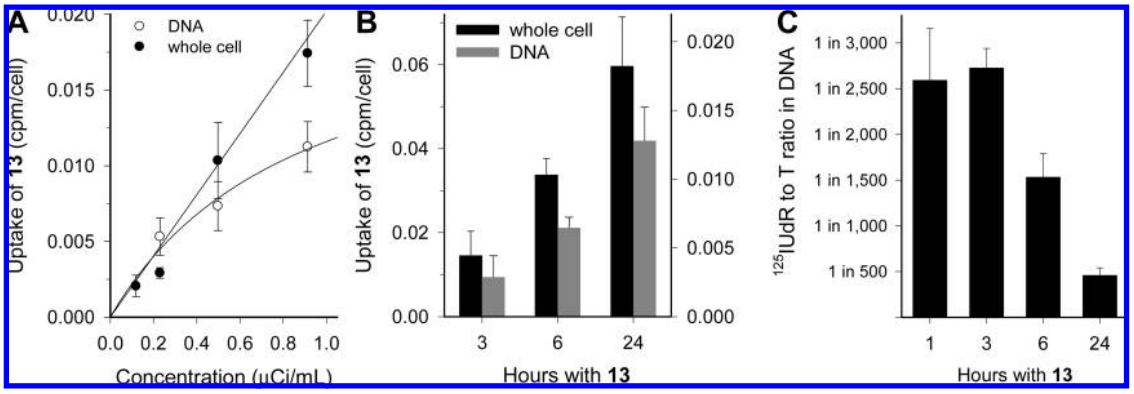

Figure 7. Uptake and subcellular distribution of **13** in NIH:OVCAR-3 human ovarian adenocarcinoma cells, which express high levels of AR. (A) Concentration dependent uptake and DNA incorporation of **13** in OVCAR-3 cells after 24 h with the drug followed by additional 24 h of continued culture in fresh complete RPMI-1640 medium. (B) Time-dependent uptake of **13** used at a concentration of 1.75 μCi/mL in OVCAR-3 cells. At designated times, radioactive medium was replaced with fresh medium and cells were cultured for an additional 48 h. Left *y*-axis is the total cell uptake; right *y*-axis represents the DNA uptake, both in cpm/cell. (C) Thymidine replacement by ^{125}IUdR in DNA of OVCAR-3 cells treated with **13**.

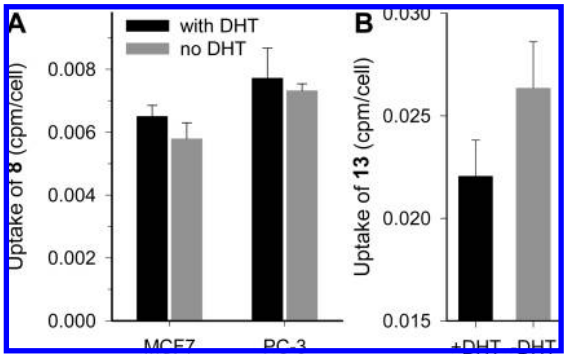

Figure 8. (A) Uptake of **8** in MCF7 and PC-3 cells, two cell lines with very low or no AR expression, grown in the presence of 0.1 μCi/mL **8** with (black) or without (gray) 0.1 μM DHT at 4 °C for 16 h. (B) Uptake of **13** in LNCaP cell grown for 48 h with (black) and without (gray) 1 μM DHT.

uptake,[53,54] resulting in high levels of ^{125}I incorporation into the DNA (Figure 7B and Figure 7C). This favorable characteristic of **13** is evident in the concentration- (Figure 7A) as well as time-dependent uptake and the corresponding subcellular fractionation studies (Figure 7B). The ratio of ^{125}IUdR to thymidine in DNA is well within the cytotoxic range[49−52] with approximately 1 in 500 thymidine residues replaced by ^{125}IUdR after 24 h (Figure 7C).

MCF-7 cells, which have marginal expression of AR,[47,48,55] and PC-3 cells, which do not express AR,[45,56,57] retain only low levels of radioactivity. To verify that the uptake of intact radioactive drugs is dependent on AR expression, the uptake studies were conducted at 4 °C to prevent proliferation-dependent uptake (Figure 8). One set of cells was treated with nonradioactive DHT prior to the addition of the radioactive drug to block binding of **8** to AR. In neither PC-3 nor MCF-7 cells was the cellular retention of **8** influenced by the presence of competitor (Figure 8A). For comparison, the effect of 1 μM DHT in AR-expressing LNCaP cells is shown in Figure 8B. LNCaP cells take up ~30% more **13** in the absence of DHT.

The dissimilar effects of **8** and **13** in cancer cells, which express AR, is best observed in the cell survival studies (Figure 9). When cells are exposed to ^{125}I-**8** for 24 h, ~95% cells survive the treatment (Figure 9A, black circles). The cell killing by ^{123}I-**8** is better. After 24 h of this treatment, over 20% of cells are dead at the highest concentration (Figure 9A, white circles). This difference in the cell sensitivity to ^{125}I-**8** and ^{123}I-**8** reflects the number of decays accumulated within 24 h of the exposure to the drug. ^{123}I half-life is 13.2 h compared to 60 days for ^{125}I. Over a period of 24 h, >70% ^{123}I decays, while during the same time only 1.1% of ^{125}I is decayed. When cells are grown with ^{125}I-**8** for 48 h, their survival is reduced to ~50% at the extracellular concentration of 3 μCi/mL. Two factors contribute to this result: the accumulation of more decays and the release and reuptake of **1**. The therapeutic effectiveness of **13** is more impressive. The extracellular concentration of **13** to achieve D_{37} in LNCaP human prostate cancer cells is ~1.7 μCi/mL. Ninety percent of cells grown for 48 h in the presence of **13** at the extracellular concentration of 8 μCi/mL are dead (Figure 9C). This is attributed to the good intracellular retention of **20** released from **13** and its availability throughout the cell cycle. At any given time, in the unsynchronized cell population used in these experiments, only a fraction of cells is making DNA and can utilize **20**. The 5′-monophosphate moiety in **13** and **20** ensures their intracellular retention.[53,54]

In Vivo Studies in Athymic Mice with Intraperitoneal NIH: OVCAR-3 Xenografts. Tumor uptake and biodistribution studies were performed in immunodeficient mice bearing ip implants of OVCAR-3 cancer cells. The accumulation of the radioactivity in xenografts is evident in the whole body image (Figure 10A and Figure 10B) and biodistribution data (Figure 10C). There is a direct relationship between whole body count and the size of the tumor (data not shown). On average 8.3% ± 2.1% of the whole body radioactivity is associated with the intraperitoneal tumor as calculated from the region of interest 72 h after administration of **8** (Figure 10B). Nonadherent tumor cells and ascites lavaged from this mouse retained ~3.4% of the injected 45 μCi **8**, of which >97% was associated with cancer cells at 72 h after injection. The planar images show stomach and thyroid as the two main target tissues. Mice in this group did not receive SSKI prior to the administration of the radioactive drug; consequently, high levels of iodide-125 accumulate in thyroid and stomach.

Biodistribution data indicate that in addition to the AR-dependent tumor uptake, there is also a significant uptake of **8** in uterus (Figure 10C), with up to 1% ID/g present 72 h

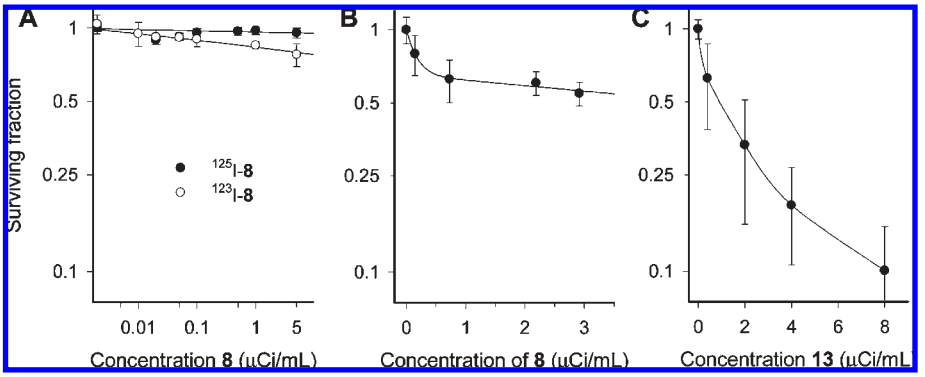

Figure 9. Survival of NIH:OVCAR-3 and LNCaP cells treated with **8** and **13**: (A) OVCAR-3 cells after 24 h with ^{125}I-**8** (black) or ^{123}I-**8** (white); (B) OVCAR-3 cells after 48 h exposure to ^{125}I-**8**; (C) LNCaP after 48 h with ^{125}I-**13**.

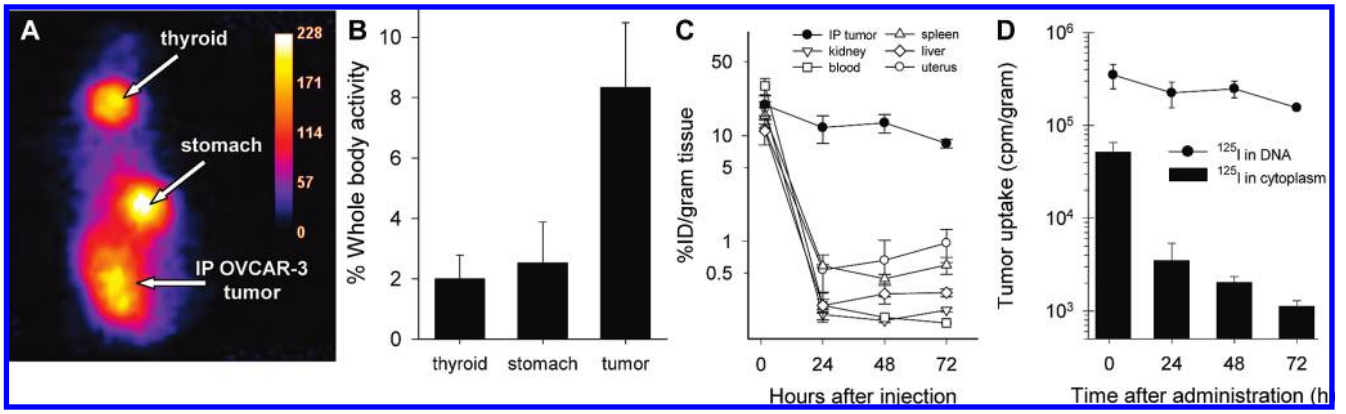

Figure 10. Biodistribution of **8** in athymic NCr-*nu*/*nu* mice bearing intraperitoneal NIH:OVCAR-3 xenografts. (A) Whole body image acquired 72 h after ip administration of 45 μCi **8**. (B) Region of interest (ROI) analyses of tumor, stomach, and thyroid uptake of **8**. ROI activities are expressed as the percent of the whole body activity. (C) Biodistribution of **8** in several normal tissues and OVCAR-3 tumor. (D) Subcellular distribution of radioactivity after ip administration of **8**. After the lavage of the peritoneal cavity, ^{125}I content was measured in whole cell, cytoplasm, and perchloric acid precipitated DNA.

after administration. Although little is known about the physiological role of AR in the mouse uterus,[58−60] recent reports indicate high expression of AR in female reproductive organs in mice.[59,60] The analysis of clearance curves shows a gradual disappearance of radioactivity with the estimated half-lives of 26 and 68 h from the peritoneal lavage and tumor cells recovered from the peritoneal cavity, respectively. At 1.5 h after ip administration of **8**, ~29% of the total peritoneal radioactivity is recovered with tumor cells. At 24 h and later, >95% of the peritoneal lavage radioactivity is associated with OVCAR-3 cells.

Therapy trials in OVCAR-3-bearing mice showed that a low dose treatment with **8**, administered either as a single ip dose of 14 μCi/mouse or as three escalating daily doses of 5, 10, and 15 μCi/mouse (total dose 30 μCi/mouse) produced only minimal tumor response. When **8** was administered in six fractionated doses every 4 days for a total dose of 180 μCi/mouse, the therapeutic effect was significant (Table 1). The number of nonadherent OVCAR-3 cells recovered in the lavage of control mice averaged 1.25×10^9 cells/mouse. Mice treated with **8** had on average 3.8×10^8 OVCAR-3 cells/mouse corresponding to ~70% reduction of the tumor size. The radioactive content of OVCAR-3 cells retrieved during the necropsy from mice treated with **8** is dose dependent (Figure 11A). All % ID/g values are corrected for decay. Tumors harvested 12 days after the last of six therapeutic doses of **8** retained ~0.5% ID/g (Figure 11A) of which ^{125}I bound to DNA, presumably in the form of ^{125}IUdR, accounts for 86.8% ± 7.4% of total cell-associated radioactivity. The treatment was far more effective in less established xenografts, i.e., when the first therapeutic dose was administered 9 or fewer days after the OVCAR-3 cancer cells implant. If before treatment tumors were allowed to grow until solid metastatic deposits were established within the peritoneum, the therapeutic effect was less. Nevertheless, 31-day-old established OVCAR-3 xenografts treated with one bolus ip dose of **13** (0.25 mCi/mouse) co-injected with SHBG produced therapeutic response, despite the apparent stimulatory effect of SHBG on the growth of OVCAR-3 xenografts[61] (Figure 11B). OVCAR-3 tumors in control mice treated with SHBG appear to grow at an accelerated rate. On the day of necropsy, 55 days after the tumor implant, the average tumor burden in SHBG-treated group was 4.1 ± 0.6 g compared to 3.7 ± 0.3 g in mice treated with PBS only. In comparison, mice treated with **13** co-injected with SHBG had a total tumor burden of 3.1 ± 0.3 g (P value of **13** + SHBG vs SHBG control was 0.19).

The main difference between tumor burden in **13** + SHBG treated mice compared to SHBG-only controls lies in the size and numbers of solid tumors (Figure 11B). Mice treated with **13** + SHBG had an average 1.2 ± 0.5 g of solid tumors, whereas the SHBG-treated mice had 1.9 ± 0.8 g of solid tumors (P = 0.021). There were also differences in the size of the nonadherent cancer cell pellet. These data, however, did not achieve statistical significance (Figure 11B, bars marked as "cells") because of the greater variability in the recovery of nonadherent tumor cells compared to solid

Table 1. OVCAR-3 Tumors Recovered from the Peritoneum of Athymic Mice after Six Fractionated ip Treatments with **8** and from Control Mice, Which Received ip Injection of Either PBS or Vehicle

	8 (×6)	treatment vehicle	PBS
average cell pellet weight (g) (SEM)	0.380(0.111)	1.702(0.172)	1.245(0.151)
median weight (g)	0.503	1.710	1.121
range of weight (g)	0.012−0.781	0.964−2.236	0.897−1.794
P for **8** vs vehicle	< 0.001		
P for **8** vs PBS	< 0.01		
P for PBS vs vehicle	> 0.05		

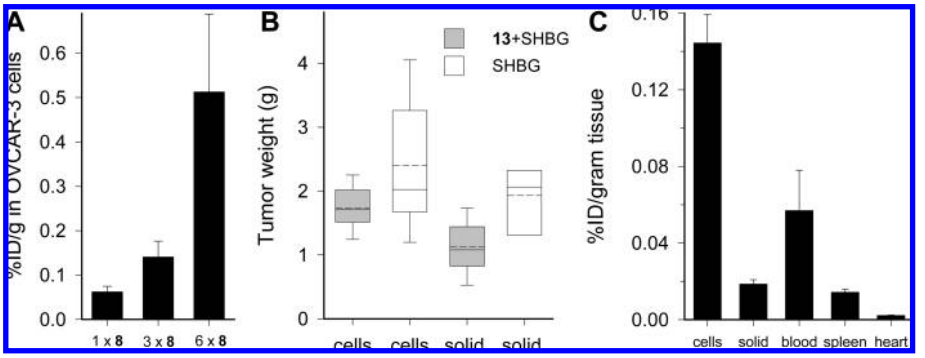

Figure 11. Necropsy results of NIH:OVCAR-3 bearing mice treated with **8** or **13**. Data were acquired at the time of termination of therapy studies. (A) Radioactivity of nonadherent OVCAR-3 cells lavaged from athymic mice treated with one, three, and six ip doses of **8**. (B) OVCAR-3 tumors recovered from the peritoneum of athymic mice after one bolus ip dose of 0.25 mCi **13** co-injected with SHBG and from control mice, which received only SHBG. "Cells" on *x*-axis refers to nonadherent OVCAR-3 cells lavaged from the peritoneum. "Solid" refers to solid tumors extirpated from these mice. Ends of the boxes define the 25th and 75th percentiles. Solid lines indicate the median. Dashed lines are the mean values. Error bars define the 10th and 90th percentiles. (C) Radioactive content of nonadherent OVCAR-3 cells, solid tumors, and several normal tissues extirpated from athymic mice treated with one dose of 0.25 mCi **13** co-injected with SHBG. % ID/g values are corrected for decay.

tumors. Moreover, 3 out of 10 mice in the control SHBG-treated group had to be terminated prematurely (4 and 2 days earlier) because of rapidly developing massive ascites. These control mice were not included in data analyses.

The necropsy of mice treated with a bolus dose of **13** revealed that the radioactivity in blood was >2.5× lower than in cancer cells at 0.057 ± 0.021% ID/g (Figure 11C). Hemoglobin (Hb) and hematocrit (Ht) values reflected the overall health on mice. Tumor-bearing control mice, which received ip injections of either PBS or vehicle, had Hb and Ht of 13.4 ± 2.2 and 58.4 ± 0.9, respectively, compared to Hb of 11.5 ± 1.3 and Ht of 51.4 ± 1.6 in mice injected with SHBG. Mice from the therapy group had Hb of 12.2 ± 1.7 and Ht of 55.2 ± 5.7. The decline in Hb levels of SHBG control mice is most likely the result of the large tumor burden. These hematologic data also suggest that **13** given at 0.25 mCi dose produces no overt adverse effects.

Therapy studies using **13** were also conducted using the fractionation scheme similar to the above described therapy study with **8**. Tumor necropsy data are summarized in Table 2. In this treatment regimen, the response of OVCAR-3 to **13** is significantly better compared to a bolus treatment with **13** as well as to the fractionated treatment with **8** ($P = 0.030$). Tumor uptake was measured at 2.9 ± 0.5% ID/g tumor. Virtually all radioactivity associated with surviving cancer cells was recovered with DNA. The average retention of ^{125}I in OVCAR-3 cells was 0.0124 ± 0.0024 cpm/cell, which corresponds to >2000 molecules of ^{125}IUdR per cell. The normal tissue uptake and in mouse bearing ip OVCAR-3 and healthy mice is shown in Table 3. In both groups of mice, the normal tissue uptake is low with the exception of spleen and uterus (also observed in mice treated with **8**). The significant presence of radioactivity in uterus is related to the expression of AR in this organ.[59,60] All tissues from tumor-bearing mice had higher radioactivity compared to control healthy mice. The slow release of ^{125}I from dying cancer cells is the likely factor responsible for these differences.

Table 2. OVCAR-3 Tumors Recovered from the Peritoneum of Athymic Mice after Six Fractionated ip Treatments with **13** and from Control Mice, Which Received ip Injection of PBS[a]

	13 (×6)	PBS
average cell pellet weight (g) (SEM)	0.061(0.006)	1.127(0.087)
median weight (g)	0.064	1.071
range of weight (g)	0.044−0.076	1.042−1.267

[a] *P* value for **13** vs PBS < 0.0001.

Discussion

Many human cancers express their highest AR levels at the refractory stage and in the metastatic deposits.[1−22,62,63] While in breast and ovarian cancers the role of AR is still only marginally defined, in prostate cancer[5−10] the expression of AR is much better understood. Recent studies demonstrate that AR can predict response to the androgen deprivation therapy[62−65] and that AR expression plays a role in the racial differences in prostate cancer mortality.[64] Development of the AR-based cancer treatments and characterization of the AR role in cancer etiology will require substantial improvements in methods used to determine tumor-associated AR levels. The noninvasive assessment of the AR expression remains a challenge. Typically, AR is measured in biopsy samples using immunohistochemistry and ex vivo biochemical assays. Both methods provide only a glimpse of the heterogeneous tumor site.

There is an ongoing effort to develop noninvasive nuclear molecular imaging methods to improve the AR assessment and, by this means, to establish the prognostic value of

Table 3. Biodistribution of OVCAR-3-Bearing Mice and Healthy Mice Treated with Fractionated ip Doses of Compound **13**

	percent injected dose per gram of tissue	
	OVCAR-3 mice	control mice
blood	0.003(0.0010)	0.001(0.0001)
lung	0.008(0.0018)	0.004(0.0007)
heart	0.003(0.0004)	0.002(0.0003)
liver	0.017(0.0020)	0.006(0.0005)
spleen	0.043(0.0103)	0.025(0.0025)
kidney	0.013(0.0063)	0.005(0.0005)
uterus	0.027(0.0051)	0.015(0.0011)
stomach	0.009(0.0010)	0.007(0.0002)
small intestine	0.011(0.0014)	0.006(0.0016)
large intestine	0.008(0.0009)	0.005(0.0009)
tumor	2.892(0.5317)	

AR.[66−72] Drugs described here contribute to this effort in several significant ways. Compounds **8** and **13** are preferentially taken up by cancer cells expressing AR in a concentration- and time-dependent manner. Both compounds bind to SHBG. When **8** and **13** are bound to SHBG in human and rabbit serum, their stability is significantly enhanced with half-lives of hours. In comparison, mouse serum, which does not contain SHBG, degrades **8** to **1** in < 10 min.

Although reports on the role of SHBG in the transport of testosterone and other hormones are conflicting,[73−77] the emerging sense is that imaging reagents with affinity to SHBG will have improved uptake in the AR expressing tumors.[78] Drugs bound to SHBG maintain higher circulating levels, permitting more than just the first-pass extraction into the tumor site. Moreover, recent evidence indicates that SHBG plays a local and more direct role in the cellular uptake of steroids than previously considered.[74,76,77] SHBG also participates in the cell signaling mechanisms triggered via a specific SHBG receptor.[73,77,76,79] On the basis of the data presented above, it is apparent that in cancer patients' blood, **8** and **13** bound to SHBG should be stable for several hours.

Upon reaching tumor cells expressing SHBG receptor or AR, the radioactive drug bound to SHBG can form a complex with SHBG receptor or can dissociate and bind to membrane AR. In either case the complex is translocated into the cancer cell presumably via the receptor-mediated endocytosis.[73,77,80] This event is particularly relevant to the therapy with **13**, which once internalized remains trapped within the cell and is available for uptake whenever the DNA synthesis commences. Since both reagents liberate metabolites able to participate in the DNA synthesis, their utility extends beyond the AR imaging. Drug **8**, which does not stay within the cell for prolonged periods, will be more useful as the AR imaging reagent. Its intracellularly released metabolite **1** will provide a snapshot of the tumor proliferation fraction. Drug **13** with its monophosphate residue, once transported into the cell, will remain there, trapped and slowly releasing **20**. In turn, compound **20** is incorporated into DNA, wherein it decays, depositing therapeutic doses of radiation and ultimately killing the cancer cell. This concept is summarized in Chart 1.

The model of SHBG interaction with its receptor in the AR-expressing cells is adopted from published data.[74,77−81] The intervention of membrane AR (mAR) in the cellular uptake is responsible for the nongenomic, rapid effects of sex steroids.[82−86] This subpopulation of AR, localized within the cell membrane, mediates the activity of ion channels and intracellular calcium levels. LNCaP cells, almost instantly after the addition of DHT,[83−85] have increased intracellular

Chart 1. Schematic Representation of Pathways Leading to the DNA Uptake of **8** and **13**[a]

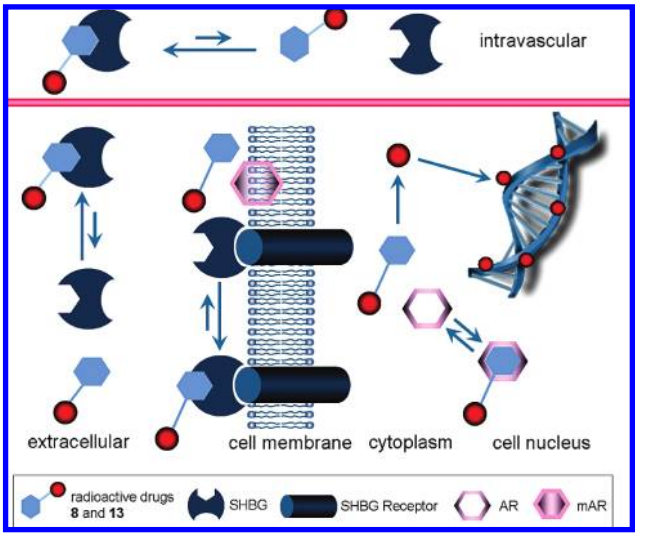

[a] SHBG has two distinct binding sites; one interacts with radioactive drugs, the second binds to the SHBG receptor in the cancer cell membrane. Dissociated drugs bind mAR. Translocated complexes release radioactive drugs and bind to intracellular AR. Unbound intracellular drugs are metabolized to **1** and **20**, which participate in DNA synthesis.

Ca^{2+} levels, and rapid activation of extracellular signal-related kinases 1 and 2 is observed. This suggests signaling through mAR. Aggressive and higher histopathological grade prostate carcinomas preferentially express mAR.[86] Compound **8** has properties ideal for imaging of mAR.

Adult mice livers do not produce SHBG. For this reason, the evaluation of anticancer drugs, which interact with SHBG, including **8** and **13** described in this study, in an animal model lacking this protein is not optimal. The therapeutic effect of **13** cannot be fully assessed in the absence of SHBG. The stimulatory effect of SHBG on the growth of ip OVCAR-3 xenografts[61] masks a significant proportion of the tumor response to **13**. Moreover, compound **13** is negatively charged and, unlike **8**, is unable to freely cross the cell membrane. Nevertheless, until athymic or SCID mice expressing SHBG become available, data derived from studies conducted in mice lacking SHBG will remain the mainstay in the evaluation of various anticancer drugs. This laboratory's efforts are directed toward the development of immunodeficient mice that produce SHBG.

Chemical structures of compounds **8** and **13** provide an unprecedented degree of flexibility in terms of the choice of radionuclides and the imaging modality, e.g., iodine-123 or iodine-131 for SPECT, and iodine-124, bromine-76, or fluorine-18 for PET imaging. Moreover, these drugs radiolabeled with either iodine-125 or iodine-124 can be used for the cancer specific delivery of lethal doses of radiation while sparing normal tissues. Iodine-124 decays via the electron capture producing, in addition to the positron emission, ~1.5 Auger electrons per transition, and therefore, it is well suited for endoradiotherapy. The amount of ^{125}I incorporated into the DNA of OVCAR-3 and LNCaP cancer cells is well within the range of D_{37} values reported for other mammalian cells.[87,88]

Conclusions

Radioactive drugs **8** and **13** have properties desired in AR imaging radiopharmaceuticals. They bind to SHBG, which

confers significant improvements to the drug stability in human serum. The in vitro uptake in cancer cells depends on the presence of AR. During the intracellular degradation of **8** and **13**, metabolites 5-^{125}I-iodo-2′-deoxyuridine **1** and its 5′-monophosphate **20** are liberated. These metabolites participate in the DNA synthesis, providing the opportunity for the simultaneous evaluation of the AR status and tumor cell proliferation. The intracellular trapping of **13** and release of **20** allow the site-specific delivery of lethal doses of radiation to cancer cells.

Experimental Section

Chemistry. Chemicals and reagents were purchased from commercial suppliers and used without further purification. Diethyl ether was dried over sodium/benzophenone and distilled under nitrogen. Pyridine, dichloromethane, and acetonitrile were distilled from calcium hydride under nitrogen. Acetonitrile for the HPLC was obtained from Fisher (HPLC grade). [^{125}I]NaI in 1×10^{-5} NaOH (pH 8−11) was obtained from PerkinElmer. Radioactivity was measured with a Minaxi γ-counter (Packard, Waltham, MA) and a dose calibrator (Capintec Inc., Ramsey, NJ). Analytical TLC was carried out on precoated plastic plates, normal phase Merck 60 F_{254} with a 0.2 mm layer of silica, and spots were visualized with either short-wave UV or iodine vapors. Radioactive drugs on TLC and ITLC plates were analyzed on a Vista-100 plate reader (Radiomatic VISTA model 100, Radiomatic Instruments & Chemical Co., Inc., Tampa, FL). Flush column chromatography was carried out using Merck silica gel 60 (40−60 μM) as stationary phase. Compounds were resolved, and their purity was confirmed by the HPLC analyses on Gilson (Middleton, WI) and ISCO (Lincoln, NE) systems using 5 μm, 250 mm × 4.6 mm, analytical columns, either Columbus C8 (Phenomenex, Torrance, CA) or ACE C18 (Advanced Chromatography Technologies, www.ace-hplc.com). Columns were protected by guard filters and were eluted at a rate of 0.8 mL/min with various gradients of CH_3CN (10−95%) in water, with or without TFA (0.07%, w/v). Variable wavelength UV detectors UVIS-205 (Linear, Irvine, CA) and UV116 (Gilson) were used with the sodium iodide crystal Flow-Count detector (Bioscan, Washington, DC) connected in-line at the outlet of the UV detector. Both signals were monitored and analyzed simultaneously. NMR spectra were recorded at ambient temperature in $(CD_3)_2SO$ or $CDCl_3$ with a Varian INOVA 500 MHz NMR instrument spectrometer (Palo Alto, CA). Chemical shifts are given as δ (ppm) relative to TMS as internal standard, with J in hertz. Deuterium exchange and decoupling experiments were performed in order to confirm proton assignments. ^{31}P NMR and ^{119}Sn NMR spectra were recorded with proton decoupling. High resolution (ESI-HR) positive ion mass spectra were acquired on an LTQ-Orbitrap mass spectrometer with electrospray ionization (ESI). Samples were dissolved in 70% methanol. Aliquots (2 μL) were loaded into a 10 μL loop and injected with a 5 μL/min flow of 70% acetonitrile and 0.1% formic acid. FAB high-resolution (FAB-HR) mass spectra analyses (positive ion mode, 3-nitrobenzyl alcohol matrix) were performed by the Washington University Mass Spectrometry Resource (St. Louis, MI) and at the University of Nebraska Mass Spectrometry Center (Lincoln, NE).

All target compounds were found to be ≥98% pure by rigorous HPLC analysis, with the integration of peak area (detected at 254 and 280 nm). Radioiodinated products were identified and evaluated by means of the independently prepared nonradioactive reference compounds. A comparison of UV signals of the nonradioactive standards with the radioactive signals using radio-TLC (R_f) and radio-HPLC (t_R) analyses was employed. Analytical HPLC traces and detailed analysis of compounds **5**−**20** are provided in Supporting Information. Dihydrotestosterone 17β-succinate was prepared according to the previously published procedure.[37] 5-Iodo-3′-*O*-levulinyl-2′-deoxyuridine **4** was prepared from 5-iodo-5′-*O*-(4,4′-dimethoxytrityl)-2′-deoxyuridine **2** in two steps: the protection of 3′-position with 4-oxopentanoic acid (DCC/DMAP in CH_2Cl_2) followed by the purification on a silica gel column ($CHCl_3/CH_3OH$, 10:0.4, 81% yield) and subsequent cleavage[89] of the DMTr group with $ZrCl_4$ in CH_3CN and a silica gel column purification ($CHCl_3/CH_3OH$, 10:0.8, 91% yield).

5-Iodo-*O*,*O*′-(di-*tert*-butyl)-2′-deoxyuridine-5′-yl Monophosphate (5). Method I. Di-*tert*-butyl *N*,*N*-diisopropylphosphoramidite (1.07 mL, 3.37 mmol), dissolved in CH_3CN (5 mL), was added gradually to a solution of 5-iodo-3′-*O*-levulinyl-2′-deoxyuridine **4** (1.22 g, 2.7 mmol) and 1*H*-tetrazole (1.12 g, 16 mmol) in acetonitrile (20 mL) at 0 °C and under nitrogen atmosphere. The reaction mixture was stirred 3 h at 0 °C, and the reaction progress was monitored by TLC (CH_2Cl_2/CH_3OH, 10:0.4). Subsequently, a 5−6 M solution of *tert*-butyl hydroperoxide (2.35 mL, ≥11.75 mmol) in *n*-decane was added at 0 °C. The solution was slowly warmed to ambient temperature and further stirred for 1 h (TLC monitoring). The solvent was removed under vacuum, and chloroform (60 mL) was added to the oily residue. The organic phase was washed with 0.3% aqueous solution of $NaHSO_3$ (20 mL) and brine (20 mL), dried over $MgSO_4$, and evaporated. The resulting crude product was partially purified by filtration through a thin pad of silica (EtOAc/hexanes, 1:1) and afforded 1.11 g of a yellow-brown solid (R_f = 0.62). This solid was dissolved in pyridine (2 mL) and added to a stirred solution of hydrazine hydrate (1.5 mL) in pyridine (3 mL) and acetic acid (2.2 mL), cooled on an ice−water bath. After 5 min of continuous stirring, water (40 mL) and ethyl acetate (50 mL) were added. The organic layer was washed with 10% aqueous $NaHCO_3$ (20 mL), water (20 mL) and dried over $MgSO_4$. TLC analyses showed a single major band (R_f = 0.32) and traces of the starting material (R_f = 0.62). The solvent was evaporated under reduced pressure, and the resulting crude product was purified by column chromatography ($CHCl_3/CH_3OH$, 10:(gradient 0.4−0.7)) to yield **5** (0.94 g, 64%) as a colorless foam. HPLC analyses: t_R = 25.05 min (99.2% pure at 254 nm) on the C18 column, eluent, solvent A 10% CH_3CN in water, solvent B CH_3CN, a linear gradient of B 0−95% over 45 min, then 95% B for 45 min; t_R = 30.3 min (99.6% pure at 280 nm) on the C8 analytical column, eluent, 25% CH_3CN isocratic. ^{1}H NMR ($CDCl_3$) δ 9.49 (bs, 1H, NH), 7.96 (s, 1H, H6), 6.23 (t, 1H, H1′, J = 6.5 Hz), 4.56−4.53 (m, 1H, H3′), 4.35−4.32 (m, 1H, H4′), 4.21−4.17 (m, 2H, H5′), 4.32 (m, 1H, OH), 2.49 (ddd, 1H, H2′′), 2.36 and 2.34 (2s, 2 × 9H, 2 × *t*-Bu), 2.24 (ddd, 1H, H2′). ^{13}C NMR ($CDCl_3$) δ 161.78 (C4), 149.32 (C2), 137.86 (C6), 112.51 (C5), 89.43 (C4′), 84.71 (C1′), 84.23 (C3′), 69.66 (C5′), 58.67 (C2′), 39.59 (C1-*t*-Bu), 29.81 (C2-*t*-Bu). ^{31}P NMR ($CDCl_3$) δ −2.87 (s). MS FAB-HR (*m*/*z*): $[M + Li]^+$ calcd for $C_{17}H_{28}N_2O_8PILi$, 553.0788, found 553.0763.

Method II. To a stirred solution of dried 5-iodo-2′-deoxyuridine **1** (1.50 g, 4.23 mmol) dissolved in a mixture of DMF/THF (15 mL, 3:4 v/v) under a nitrogen atmosphere, di-*tert*-butyl *N*,*N*-diisopropylphosphoramidite (1.65 mL, 5.23 mmol) and 1*H*-tetrazole (1.24 g, 17.7 mmol) were added at −20 °C. The reaction mixture was warmed to −4 °C and further stirred for 6 h with TLC monitoring (CH_2Cl_2/CH_3OH, 10:0.7). After the mixture was cooled to −20 °C, a 5−6 M solution of *tert*-butyl hydroperoxide in *n*-decane (2.6 mL, ≥13 mmol) was added. The solution was warmed to ambient temperature, and stirring continued for 1 h (TLC monitoring). The solvent was removed by rotary evaporation under vacuum, and the resulting crude mixture was separated and purified on a silica gel column ($CHCl_3/CH_3OH$, 10:(gradient 0.3−0.7)). The corresponding three phosphotriesters of IUdR **1** were isolated as follows: 3′,5′-diphosphotriester (R_f = 0.78), 0.47 g (15% yield); 3′-phosphotriester (R_f = 0.47), 0.78 g (34% yield); 5′-phosphotriester **5** (R_f = 0.32) corresponding to the slowest band on TLC,

1.1 g (48% yield). All products formed a colorless foam upon evaporation of the solvent. The analytical data of product **5** produced in method II were identical to these reported above for method I.

5-Iodo-3′-*O*-(17*β*-succinyl-5α-androstan-3-one)-2′-deoxyuridine (6). To a stirred solution of dihydrotestosterone 17*β*-succinate (0.82 g, 2.10 mmol), 5-iodo-5′-*O*-(4,4′-dimethoxytrityl)-2′-deoxyuridine **2** (1.45 g, 2.21 mmol), and 4-dimethylaminopyridine (0.05 g, 0.41 mmol) in dry dichloromethane (25 mL) at 0 °C, 1,3-dicyclohexylcarbodiimide (0.50 g, 2.42 mmol) was added. After 1 h, the solution was allowed to warm to room temperature and stirring continued for an additional 4 h (TLC monitoring). The solvent was removed under vacuum, and a residue dissolved in diethyl ether (80 mL) was filtered. The filtrate was washed with a 5% solution of citric acid (20 mL), 10% $NaHCO_3$ (20 mL), and water (2 × 20 mL) and dried over $MgSO_4$. The solvent was evaporated under reduced pressure. The resulting crude product was purified by repeated column chromatography (ethyl acetate/hexanes, 3:(gradient 2−1)) to yield 5′-DMTr-protected **6** (1.84 g, 81%) as a colorless foam. TLC: R_f = 0.64 (ethyl acetate/hexanes, 3:2). ^{1}H NMR ($CDCl_3$) δ 8.76 (bs, 1H, NH), 8.15 (s, 1H, H6), 7.48−7.21 (m, 5H, aryl; 4H, 2 × H2-arylOMe; 2 × H6-arylOMe), 6.87−6.84 (m, 4H, 2 × H3-arylOMe, 2× H5-arylOMe), 6.34 (dd, 1H, H1′), 5.51−5.48 (m, 1H, H3′), 4.64 (t, 1H, H17-DHT, J = 8.5 Hz), 4.17−4.15 (m, 1H, H4′), 4.13−3.98 (m, 2H, H5′), 3.79 (s, 6H, 2×OCH_3-DMTr), 2.67−2.61 (m, 4H, H2 and H3 succinyl), 2.55 (ddd, 1H, H2″), 2.41 (ddd, 1H, H2′), 2.31−0.68 (m, 28H, from DHT with 1.01(s), 3H, H18-DHT and 0.799 (s), H19-DHT). MS FAB-HR (m/z): $[M + H]^+$calcd for $C_{53}H_{62}N_2O_{11}I$, 1029.9707, found 1029.9697. To a stirred solution of 5′-DMTr-protected **6** (1.51 g, 1.47 mmol) dissolved in 2-propanol (12 mL), a solution of 90% aqueous TFA (1 mL) was added, and stirring continued for 2 h (TLC monitoring). The solvent was evaporated under vacuum, 10 mL of water added, and the evaporation continued to remove TFA. The water layer was extracted with dichloromethane (2 × 25 mL), and combined extracts were dried over $MgSO_4$. Solvent was removed by rotary evaporation under reduced pressure, and the resulting crude product was purified by column chromatography (CH_2Cl_2/ethyl acetate, 3:2) to yield **6** (1.17 g, 73% overall yield from **4**) as a rigid foam. HPLC analyses: t_R = 19.1 min (≥98% pure at 254 nm) on the C18 analytical column, eluent, solvent A 50% CH_3CN, solvent B CH_3CN, with a linear gradient of B 0−95% over 30 min, then 95% B for 30 min; t_R = 23.4 min (99.3% pure at 280 nm) on the C8 analytical column, eluent, 50% CH_3CN isocratic. TLC: R_f = 0.31 (CH_2Cl_2/ethyl acetate, 3:2), R_f = 0.26 (CH_2Cl_2/CH_3OH, 10:0.5). ^{1}H NMR ($CDCl_3$) δ 8.64 (bs, 1H, NH), 8.31 (s, 1H, H6), 6.26 (dd, 1H, H1′), 5.40−5.38 (m, 1H, H3′), 4.62 (t, 1H, H17-DHT, J = 8.5 Hz), 4.15−4.10 (m, 1H, H4′), 3.99−3.92 (m, 2H, H5′), 2.69−2.64 (m, 4H, H2- and H3-succinyl), 2.49 (ddd, 1H, H2″), 2.38 (ddd, 1H, H2′), 2.27−0.85 (m, 28H, from DHT with 1.02 (s), 3H, H18-DHT and 0.81 (s), 3H, H19-DHT). MS FAB-HR (m/z): $[M + Li]^+$calcd for $C_{32}H_{43}N_2O_9ILi$ 733.5375, found 733.5341.

5-Iodo-3′-*O*-(17*β*-succinyl-5α-androstan-3-one)-*O*,*O*′-(di-*tert*-butyl)-2′-deoxyuridin-5′-yl Monophosphate (9). Method I. Di-*tert*-butyl *N*,*N*-diisopropylphosphoramidite (755 μL, 2.39 mmol) dissolved in CH_3CN (3 mL) was added to a solution of 5-iodo-3′-*O*-(17*β*-succinyl-5α-androstan-3-one)-2′-deoxyuridine **6** (1.39 g, 1.91 mmol) and 1*H*-tetrazole (0.67 g, 9.56 mmol) in CH_3CN (10 mL) at 0 °C under the nitrogen atmosphere. The reaction mixture was stirred for 4 h at 0 °C. The slow progress of the reaction was monitored by TLC (CH_2Cl_2/CH_3OH, 10:05). The mixture was left under nitrogen at 4 °C overnight. Subsequently, 5−6 M *tert*-butyl hydroperoxide in *n*-decane (2.1 mL, ≥10.5 mmol) was added at 0 °C. The resulting mixture was slowly warmed to ambient temperature and further stirred for 1 h (TLC monitoring). The solvent was removed under vacuum. Chloroform (60 mL) was added to the remaining oily residue. The organic phase was washed with a 0.3% aqueous solution of $NaHSO_3$ (20 mL) and brine (20 mL), dried over $MgSO_4$, and evaporated. The crude product was purified on a silica gel column (CH_2Cl_2/CH_3OH, 10:0.4) to give **9** (0.193 g, 11%) as a colorless foam. HPLC analyses: t_R = 26.6 min (99.2% pure at 254 nm) on the C18 analytical column, eluent, as for **6**; t_R = 59.8 min (≥98% pure at 280 nm) on the C8 analytical column, eluent, 50% CH_3CN isocratic. TLC: R_f = 0.62 (ethyl acetate), R_f = 0.22 ($CHCl_3$/CH_3OH, 10:0.4). ^{1}H NMR ($CDCl_3$) δ 8.74 (bs, 1H, NH), 8.10 (s, 1H, H6), 6.32 (dd, 1H, H1′), 5.37 (d, 1H, H3′), 4.62 (t, 1H, H17-DHT, J = 8.5 Hz), 4.31−4.29 (m, 1H, H4′), 4.21−4.12 (m, 2H, H5′), 2.71−2.61 (m, 4H, H2 and H3 succinyl), 2.49 (ddd, 1H, H2″), 2.39 (ddd, 1H, H2′), 2.32−0.75 (m, 28H, from DHT with 1.12 (s), 3H, H18-DHT, 0.82 (s), 3H, H19-DHT and 1.53 (s), 18H, 2×*t*-Bu). ^{31}P NMR ($CDCl_3$) δ −9.90 (s). MS FAB-HR (m/z): $[M + Li]^+$ calcd for $C_{40}H_{60}N_2O_{12}PILi$ 925.3089, found 925.3142.

Method II. To a stirred solution of dihydrotestosterone 17*β*-succinate (0.72 g, 1.84 mmol) and 5-iodo-*O*,*O*′-(di-*tert*-butyl)-2′-deoxyuridin-5′-yl phosphate **5** (1.05 g, 1.92 mmol) containing 4-dimethylaminopyridine (0.065 g, 0.53 mmol) in dry dichloromethane (35 mL) at 0 °C, 1,3-dicyclohexylcarbodiimide (0.40 g, 1.93 mmol) was added. The solution was warmed slowly to room temperature, and stirring continued for an additional 6 h (TLC monitoring). The mixture was diluted with *n*-hexane (40 mL) and filtered. The filtrate was washed consecutively with 5% aqueous citric acid (20 mL), 10% $NaHCO_3$ (20 mL), and water (2 × 20 mL) and dried over $MgSO_4$. The solvent was removed under reduced pressure. The resulting crude product was purified by repeated column chromatography ($CHCl_3$/CH_3OH, 10:(a gradient of 0.2−0.4)) to yield **9** (1.17 g, 69%) as a colorless foam. The analytical data were identical to these reported above for product prepared by method I.

Method III. To a solution of dihydrotestosterone 17*β*-succinate (0.56 g, 1.43 mmol) in dry dichloromethane (15 mL), *N*,*N*′-carbonyldiimidazole (0.30 g, 1.79 mmol) was added under a nitrogen atmosphere. The tightly closed reaction flask was fitted with a septum allowing for gas expansion. The mixture was kept at 4 °C for 1 h and then stirred at room temperature until the evolution of carbon dioxide subsided. The solution of dried 5-iodo-*O*,*O*′-(di-*tert*-butyl)-2′-deoxyuridin-5′-yl phosphate **5** (0.83 g, 1.52 mmol) in dry dichloromethane (5 mL) was added via a syringe, followed by the addition of sodium amide (200 μL) as a (5% w/v) suspension in toluene. The mixture was stirred for 5 h at 40 °C (TLC monitoring). The mixture was diluted with dichloromethane (50 mL) and filtered. The filtrate was washed consecutively with 5% aqueous citric acid (20 mL) and water (2 × 20 mL) and dried over $MgSO_4$. The resulting crude product was purified on a silica gel column ($CHCl_3$/CH_3OH, 10:0.4) to give **9** (0.91 g, 65%) as a colorless foam. The analytical data were identical to these reported above for product prepared by method I.

5-Iodo-3′-*O*-(17*β*-succinyl-5α-androstan-3-one)-2′-deoxyuridin-5′-yl Monophosphate (14). Phosphotriester **9** (0.67 g, 0.73 mmol), dried by repeated coevaporation with anhydrous acetonitrile under anhydrous nitrogen followed by brief high vacuum drying (15 min, ∼0.05 mmHg) was dissolved in anhydrous acetonitrile (5 mL). TFA (0.9 mL) was added at room temperature. The reaction progress was monitored by TLC (concentrated ammonia/water/2-propanol, 2:1:3), showing three bands with R_f values of 0.69 (traces of starting **9**), 0.27, and 0.19 (major). After 40 min of hydrolysis, the band with R_f = 0.27 was no longer detected. The solvent was removed by rotary evaporation under reduced pressure, and the residue was coevaporated with water (3 × 20 mL) at 50 °C, 15 mmHg. The residue was then dried under vacuum and suspended in anhydrous diethyl ether (15 mL). A formed white powder was decanted, dried again, and dissolved in acetonitrile (3 mL). Slow addition of anhydrous diethyl ether (∼1.2 mL) caused the precipitation of **14** (0.42 g, 71%) in the form of a white amorphous solid. HPLC analyses: t_R = 10.2 min (≥96% pure at 254 nm) on the C18 analytical column, eluent, solvent A 50% CH_3CN, solvent B CH_3CN (both containing 0.07% TFA), a linear gradient of B 0−95% over 35 min, then 95% B for 15 min; t_R = 34.8 min (≥97% pure at 254 nm) on the C18 analytical column, eluent, solvent A

0.05 M potassium phosphate buffered saline, pH 7.1 (PBS), solvent B CH_3CN, a linear gradient of B, 0−50% over 30 min, then 50% B for 30 min. ^{1}H NMR (DMSO-d_6) δ 11.74 (s, 1H, NH), 11.55−10.64 (bs, 2H, $(HO)_2P(O)-$), 8.10 (s, 1H, H6), 6.12 (dd, 1H, H1′), 5.21 (d, 1H, H3′), 4.53 (t, 1H, H17-DHT, J = 8.5 Hz), 4.25−4.13 (m, 2H, H4′), 4.10−4.03 (m, 2H, H5′), 2.64−2.56 (m, 4H, H2 and H3 succinyl), 2.48 (ddd, 1H, H2″), 2.36 (ddd, 1H, H2′), 2.34−0.76 (m, 28H, from DHT with 0.97 (s), 3H, H18-DHT, 0.78 (s), 3H, H19-DHT). ^{31}P NMR (DMSO-d_6) δ −0.19 (s). MS ESI-HR (m/z): $[M + H]^+$ calcd for $C_{32}H_{45}O_{12}N_2PI$, 807.1677, found 807.1733; $[M + Na]^+$ 829.1552.

5-Iodo-3′-*O*-succinyl-2′-deoxyuridine Ethyl Ester (15). To a stirred solution of 5-iodo-5′-*O*-(4,4′-dimethoxytrityl)-2′-deoxyuridine **2** (0.73 g, 1.11 mmol) in dry dichloromethane (7 mL), monoethyl succinate (180 μL, 1.40 mmol) and DCC (0.23 g, 1.12 mmol) were added, followed by 4-dimethylaminopyridine (20 mg, 0.16 mmol). The reaction was completed within 30 min of stirring (TLC monitoring, CH_2Cl_2/CH_3OH, 10:0.6). The reaction mixture, diluted with hexanes (10 mL), was cooled on an ice bath, filtered, washed consecutively with 5% aqueous citric acid (10 mL), 10% $NaHCO_3$ (10 mL), and water (2 × 10 mL), and dried over $MgSO_4$. The solvent was removed by rotary evaporation at 35 °C, 20 mmHg, and the oily residue was dissolved in *tert*-butanol (15 mL). To the resulting solution, 90% solution of TFA (1.8 mL) was added in portions, with constant stirring. After 2 h (TLC monitoring), the mixture was evaporated under vacuum. The resulting residue was taken up into dichloromethane (50 mL) and washed with 10% solution of $NaHCO_3$ (10 mL) and water (15 mL). The organic layer was dried over $MgSO_4$ and purified on a silica gel column (CH_2Cl_2/CH_3OH, 10:0.4) to give **15** (0.42 g, 78%) as a colorless rigid foam. HPLC analyses: t_R = 22.1 min (≥98% pure at 254 nm) on the C18 analytical column, eluent solvent A 10% CH_3CN in water, solvent B CH_3CN, a linear gradient of B, 0−95% over 40 min, then 95% B for 20 min. ^{1}H NMR ($CDCl_3$) δ 9.11 (bs, 1H, NH), 8.32 (s, 1H, H6), 6.26 (dd, 1H, H1′), 5.41 (d, 1H, H3′), 4.18−4.15 (m, 3H, H4′, H5′), 3.97 (q, 2H, H5-ethylsuccinyl), 2.67−2.64 (m, 4H, H2- and H3-ethylsuccinyl), 2.49 (ddd, 1H, H2″), 2.38 (ddd, 1H, H2′), 1.27 (t, 3H, H6-ethylsuccinyl). MS ESI-HR (m/z): $[M + H]^+$ calcd for $C_{15}H_{20}N_2O_8I$ 483.0186, found 483.0248; $[M + Na]^+$ 505.0058.

General Procedure A: Preparation of Trialkyltin Precursors 7, 10, 11, 16, and 18. A solution of appropriate iododuridine **5**, **6**, **9**, **15** (1.0 equiv), hexamethyl- or hexa-*n*-butylditin (1.25−1.50 equiv), and dichlorobis(triphenylphosphine)palladium(II) (0.10 equiv) in ethyl acetate or dioxane was refluxed (2−10 h) under a nitrogen atmosphere until the starting material disappeared. Two major products were formed in all reactions: the compound with the higher mobility on TLC isolated in 50−72% yield, which was proven to be the trialkylstannyl derivative, and the second product with lower TLC mobility, later identified as the proton deiodinated starting compound. After cooling to ambient temperature, the mixture was freed from excess catalyst and partially purified by the filtration through a thin pad of silica (EtOAc/hexanes, 2:1). The resulting crude product was purified by repeated silica gel column chromatography (EtOAc/hexanes, 2:(gradient 0.5−1), and/or $CHCl_3/CH_3OH$, 10:(gradient 0.4−0.7)). Anhydrous aliquots of pure trialkyltin precursors (120 μg/tube) were stored up to 4 months, with the exclusion of light under nitrogen at −20 °C without any evidence of excessive decomposition. All stored trialkyltin precursors were >92% pure after 4 months, as indicated by HPLC analysis, and were suitable for immediate radioiododestannylation.

5-Trimethylstannyl-3′-*O*-(17β-succinyl-5α-androstan-3-one)-2′-deoxyuridine (7). General procedure A was conducted with 5-iodo-3′-*O*-(17β-succinyl-5α-androstan-3-one)-2′-deoxyuridine **6** (0.87 g, 1.19 mmol), hexamethylditin (0.31 mL, 1.51 mmol), and palladium(II) catalyst (0.095 g, 0.135 mmol) in dioxane (35 mL) for 3 h. Purification was done by column chromatography (EtOAc/hexanes, 2:(gradient 2−1)). Product **7** (0.56 g, 61%) was obtained as a yellow foam which solidified from a mixture of ethyl acetate/hexanes upon standing. HPLC analyses: t_R = 23.9 min (≥98% pure at 254 nm) on the C18 analytical column, eluent, solvent A 50% CH_3CN, solvent B CH_3CN, a linear gradient of B 0−95% over 20 min, then 95% B for 15 min; t_R = 47.2 min, (≥99% pure at 280 nm) on the C8 analytical column, eluent, 50% aqueous CH_3CN isocratic. TLC: R_f = 0.44 (CH_2Cl_2/ethyl acetate, 3:2), R_f = 0.34 (CH_2Cl_2/CH_3OH, 10:0.5). ^{1}H NMR ($CDCl_3$) δ 8.12 (bs, 1H, NH), 7.48 (s, 1H, H6, J(Sn,H) = 19.5 Hz), 6.23 (dd, 1H, H1′), 5.-5.38 (m, 1H, H3′), 4.61 (t, 1H, H17-DHT, J = 8.5 Hz), 4.13−4.11 (m, 1H, H4′), 3.92−3.89 (m, 2H, H5′), 2.69−2.63 (m, 4H, H2-, H3-succinyl), 2.53 (ddd, 1H, H2″), 2.39 (ddd, 1H, H2′), 2.33−0.76 (m, 28H, from DHT with 1.02 (s), 3H, H18-DHT and 0.81 (s), 3H, H19-DHT), 0.29 (s), 9H, 3×CH_3, J(Sn,H) = 29.5 Hz). ^{119}Sn NMR ($CDCl_3$) δ −0.61 (s). MS FAB-HR (m/z): $[M + H]^+$ calcd for $C_{35}H_{53}N_2O_9Sn$, 765.2695, found 765.2549; $[M + Li]^+$ 771.2846.

5-Tri-*n*-butylstannyl-3′-*O*-(17β-succinyl-5α-androstan-3-one)-*O*,*O*′-(di-*tert*-butyl)-2′-deoxyuridin-5′-yl Monophosphate (10). General procedure A was conducted with 5-iodo-3′-*O*-(17β-succinyl-5α-androstan-3-one)-*O*,*O*′-(di-*tert*-butyl)-2′-deoxyuridin-5′-yl phosphate **9** (0.50 g, 0.54 mmol), hexa-*n*-butylditin (0.35 mL, 0.68 mmol), and palladium(II) catalyst (0.039 g, 0.055 mmol) in ethyl acetate (25 mL) for 9 h. Purification was accomplished by column chromatography (EtOAc/hexanes, 2:1, and $CHCl_3/CH_3OH$, 10:(gradient 0.2−0.4)). Product **10** (0.29 g, 49%) was obtained as a yellow foam after repeated coevaporation with dry CH_3CN and drying in a high vacuum. HPLC analyses: t_R = 52.03 min (≥98% pure at 254 nm) on the C18 analytical column, eluent, solvent A 50% CH_3CN, solvent B CH_3CN, linear gradient of B 0−95% over 30 min, then 95% CH_3CN for 60 min; t_R = 22.6 min (≥99% pure at 280 nm) on the C8 column, eluent, 90% CH_3CN isocratic. TLC: R_f = 0.68 (ethyl acetate/hexanes, 3:1), R_f = 0.36 ($CHCl_3/CH_3OH$, 10:0.4). ^{1}H NMR ($CDCl_3$) δ 8.02 (s, 1H, NH), 7.22 (s, 1H, H6, J(Sn,H) = 16.5 Hz), 6.22 (dd, 1H, H1′), 5.36 (d, 1H, H3′), 4.62 (t, 1H, H17-DHT, J = 8.5 Hz), 4.26−4.23 (m, 2H, H4′, H5″), 4.18−4.05 (m, 1H, H5′), 2.65−2.44 (m, 4H, H2 and H3 succinyl), 2.46 (ddd, 1H, H2″), 2.36 (ddd, 1H, H2′), 2.34−0.74 (m, 28H, from DHT with 1.02 (s), 3H, H18-DHT, 0.88 (s), 3H, H19-DHT, overlapped with 1.49 (s), 9H, *t*-Bu 1.47 and (s), 9H, *t*-Bu, 1.58−1.44 (m), 6H, 3×H1-*n*-Bu, 1.41−1.28 (m), 6H, 3×H2-*n*-Bu, 1.19−1.06 (m), 6H, 3×H3-*n*-Bu, 0.89 (t), 9H, 3×H4-*n*-Bu). ^{31}P NMR ($CDCl_3$) δ −9.41(s). MS FAB-HR (m/z): calcd for $C_{52}H_{88}N_2O_{12}PSn$ 1082.5019 $[M + H]^+$, found 1082.5542; $[M + Li]^+$ 1089.5221.

5-Trimethylstannyl-3′-*O*-(17β-succinyl-5α-androstan-3-one)-*O*,*O*′-(di-*tert*-butyl)-2′-deoxyuridin-5′-yl Monophosphate (11). General procedure A was conducted with 5-iodo-3′-*O*-(17β-succinyl-5α-androstan-3-one)-*O*,*O*′-(di-*tert*-butyl)-2′-deoxyuridin-5′-yl phosphate **9** (0.54 g, 0.59 mmol) and hexamethylditin (0.29 g, 0.88 mmol) in the presence of palladium(II) catalyst (0.032 g, 0.046 mmol) in ethyl acetate (30 mL) for 2 h. The product was purified on a silica gel column (EtOAc/hexanes, 3:1, and $CHCl_3/CH_3OH$, 10:0.5). **11** (0.41 g, 72%) was obtained as a colorless rigid foam after evaporation with anhydrous CH_3CN and was dried in a high vacuum. HPLC analyses: t_R = 32.5 min (≥99% pure at 254 nm) on the C18 analytical column, eluent, solvent A 50% CH_3CN, solvent B CH_3CN with a linear gradient of B 0−95% over 30 min, then 95% CH_3CN for 30 min; t_R = 40.2 min (≥99% pure at 280 nm) on the C8 analytical column, eluent, 60% CH_3CN isocratic. TLC: R_f = 0.51 (ethyl acetate/hexanes, 3:1), R_f = 0.28 (CH_2Cl_2/CH_3OH, 10:0.4). ^{1}H NMR ($CDCl_3$) δ 8.27 (s, 1H, NH), 7.35 (s, 1H, H6, J(Sn,H) = 18.4 Hz), 6.31 (dd, 1H, H1′), 5.39 (d, 1H, H3′), 4.62 (t, 1H, H17−DHT, J = 8.5 Hz), 4.30−4.28 (m, 1H, H4′), 4.26−4.09 (m, 2H, H5′), 2.69−2.60 (m, 4H, H2 and H3 succinyl), 2.42 (ddd, 1H, H2″), 2.34 (ddd, 1H, H2′), 2.32−0.72 (m, 28H, from DHT with 1.01 (s), 3H, H18-DHT, 0.81 (s), 3H, H19-DHT, overlapped with 1.50 (s), 9H, *t*-Bu and 1.48 (s), 9H, *t*-Bu), 0.31 (s, 9H, 3×CH_3, J(Sn,H) = 29.1 Hz). ^{31}P NMR ($CDCl_3$) δ −9.81(s). MS ESI-HR (m/z): calcd for $C_{43}H_{70}O_{12}N_2PSn$ 956.3610 $[M + H]^+$, found 957.3685; $[M + Na]^+$ 979.3473.

5-Trimethylstannyl-3′-*O*-succinyl-2′-deoxyuridine Ethyl Ester (16). General procedure A was conducted with 5-iodo-3′-*O*-succinyl-2′-deoxyuridine ethyl ester **15** (0.94 g, 1.95 mmol), hexamethylditin (1.02 g, 3.12 mmol), and palladium(II) catalyst (0.021 g, 0.03 mmol) in ethyl acetate (40 mL) for 40 min to give stannane **16** (0.74 g, 73%) in the form of a colorless rigid foam after purification on a silica gel column (CH_2Cl_2/CH_3OH, 10: (gradient 0.3−0.7)) and repeated evaporation from dried acetonitrile. HPLC analyses: $t_R = 28.6$ min (≥99% pure at 254 nm) on the C18 column, eluent, solvent A 10% CH_3CN, solvent B CH_3CN, with a linear gradient of B 0−95% over 40 min, then 95% B for 20 min. TLC $R_f = 0.42$ (ethyl acetate/hexanes 3:1), $R_f = 0.33$ (CH_2Cl_2/CH_3OH, 10:0.5). ^{1}H NMR ($CDCl_3$) δ 8.58 (bs, 1H, NH), 7.49 (s, 1H, H6, J(Sn,H) = 19.0 Hz), 6.24 (dd, 1H, H1′), 5.41 (d, 1H, H3′), 4.18−4.12 (m, 3H, H4′, H5′), 3.92 (q, 2H, $COOCH_2-$), 2.67−2.63 (m, 4H, $-OCH_2CH_2O-$), 2.56 (ddd, 1H, H2″), 2.49 (ddd, 1H, H2″), 1.73(m, 1H, OH), 1.27 (t, 3H, $-CH_3$), 0.29 (s, 9H, $3 \times CH_3$, J(Sn,H) = 29.1 Hz). ^{13}C NMR ($CDCl_3$) δ 172.15 (C1,C4-succinyl), 165.93 (C4), 150.95 (C2), 144.56 (C6), 113.31 (C5), 86.79 (C1′), 85.14 (C4′), 75.32 (C3′), 62.73 (C5′), 60.92 (C2 -ethyl), 37.14 (C2′), 29.13 (C2-succinyl), 28.99 (C3-succinyl), 14.19 (C1-ethyl), −9.29 (CH_3-Sn). ^{119}Sn NMR (CDCl3) δ −0.58 (s). MS ESI-HR (m/z): calcd for $C_{18}H_{29}O_8N_2PSn$ 521.0868 $[M + H]^+$, found 521.0929; $[M + Na]^+$ 543.0749.

5-Trimethylstannyl-*O*,*O*′-(di-*tert*-butyl)-2′-deoxyuridin-5′-yl Monophosphate (18). General procedure A was carried out with 5-iodo-*O*,*O*′-(di-*tert*-butyl)-2′-deoxyuridin-5′-yl monophosphate **5** (1.22 g, 2.23 mmol) and hexamethylditin (1.25 g, 3.81 mmol) in the presence of palladium(II) catalyst (0.15 g, 0.21 mmol) in dioxane (50 mL) to give stannane **18** (0.92 g, 70%) as a colorless foam. A crude product was purified on a silica gel column (CH_2Cl_2/CH_3OH, 10:(gradient 0.5-0.9)) and twice evaporated from dried acetonitrile. HPLC analysis: t_R = 32.6 min (≥98% pure, at 254 nm), C-18 analytical column, eluent, solvent A 10% CH_3CN, solvent B CH_3CN with a linear gradient of B 0−95% over 40 min, then 95% B for 20 min. TLC $R_f = 0.32$ (ethyl acetate/hexanes, 4:1), R_f = 0.47 (CH_2Cl_2/CH_3OH, 10:0.5). ^{1}H NMR (DMSO-d_6) δ 11.19 (s, 1H, NH), 7.22 (s, 1H, H6, J(Sn,H) = 19.5 Hz), 6.17 (t, 1H, H1′, J = 6.7 Hz), 5.42 (d, 1H, OH, J = 4.4 Hz), 4.25−4.22 (m, 1H, H3′), 4.04−3.98 (m, 1H, H4′), 3.96−3.91 (m, 2H, H5′), 2.51−2.12 (m, 2H, H2′), 1.41 and 1.4 (2s, 2×9H, 2×H2-*t*-Bu), 0.22 (s, 9H, $3 \times CH_3$, J(Sn,H) = 29.5 Hz). ^{13}C NMR (DMSO-d_6) δ 166.21 (C4), 150.76 (C2), 144.01 (C6), 111.65 (C5), 90.65 (C1′), 84.67 (C4′), 81.73, 81.67 (CH_3 *t*-Bu), 70.23 (C3′), 66.24 (C5′), 40.00 (C2′), 29.40 (CH_3 *t*-Bu), 29.37 (CH_3 *t*-Bu), −9.00 (CH_3-Sn). ^{31}P NMR (DMSO-d_6) δ −8.87 (s). ^{119}Sn NMR (DMSO-d_6) δ −2.03 (s). MS ESI-HR (m/z): calcd for $C_{20}H_{38}O_8N_2PSn$ 585.1382 $[M + H]^+$, found 585.1372; $[M + Na]^+$ 607.1189.

General Procedure B: Synthesis of ^{125}I-Radioiodinated Target Compounds 8, 12, 17, and 19. Into a glass tube containing the appropriate tin precursor **7**, **10**, **11**, **16**, or **18** (100−120 μg, ∼140 μmol) dissolved in CH_3CN (50 μL), a solution of $Na^{125}I$/NaOH (10−100 μL, 1−10 mCi) was added followed by 30% H_2O_2 (5 μL) and TFA (50 μL, 0.1 N solution in CH_3CN). The mixture was briefly vortexed and left for 15 min at room temperature. The reaction was quenched with $Na_2S_2O_3$ (100 μg in 100 μL H_2O), taken up into a syringe, and the reaction tube was rinsed twice with 50 μL of H_2O/CH_3CN (9:1) solution. The reaction mixture and tube washes were combined and separated on the HPLC system by means of the C8 or C18 column. Eluant from the column (1 mL fractions were collected) was monitored using the radioactivity detector connected to the outlet of the UV detector (detection at 254 and 280 nm). Fractions containing product, combined and evaporated with a stream of nitrogen, were reconstituted in the appropriate solvent and concentration and were filtered through a sterile (Millipore 0.22 μm) filter into a sterile evacuated vial. The identities of radiolabeled products were confirmed through the evaluation of the elution of nonradioactive independently prepared iodo analogues with the radioactive signals by comparing R_f obtained from the radio-TLC and t_R from the radio-HPLC analyses. Specific activities were determined by the UV absorbance of radioactive peaks compared to standard curves of the unlabeled reference compounds. Radiolabeled products, if stored in a solution overnight at ambient temperature, were always repurified before conducting the experiments, although the HPLC indicated no less than 92% of the radiochemical purity/stability after 24 h of storage.

5-[^{125}I]Iodo-3′-*O*-(17β-succinyl-5α-androstan-3-one)-2′-deoxyuridine (8). General procedure B was used. The main radioactivity peak from the reaction mixture of **7** (100 μg) with [^{125}I]NaI/NaOH (37 μL, 3.5 mCi) was eluted from HPLC in three fractions within 18−20 min after the injection and was collected in a volume of 2.5 mL. Radioiodinated product **8** (t_R = 19.6 min) was cleanly separated from the excess of unreacted precursor **7**, which eluted 4.5 min later (t_R = 24.6 min). The average radiochemical yield calculated from six independent radioiododestannylations, conducted with the amounts of $Na^{125}I$ ranging from 1 to 10 mCi, was 89%. The product was 94% pure **8**. Inorganic iodide (∼9%) was collected in four fractions within 4−7 min of the injection. Identical methods were applied, and similar results were obtained in the radioiododestannylation of **7** with iodine-123. Analytical HPLC analyses (4 μCi **8** injected): t_R = 19.6 min (≥98% pure, Bioscan) on the C18 analytical column; conditions and solvents developed for the analysis of **6** were applied here. Additional HPLC analyses: t_R = 36.6 min (≥98% pure, Bioscan) on the C18 column, eluent, solvent A H_2O, solvent B CH_3CN, both solvents with 0.07% TFA, initial elution with A for 10 min, then a linear gradient of B, 0−95% over 30 min and 95% B for 20 min; t_R = 47.5 min (≥98% pure, Bioscan), TSK-GEL G3000SW column, eluent, solvent A a mixture (1:1, v/v) of 0.1 M potassium phosphate buffer (PB) and 0.1 M Na_2SO_4, (pH 6.8), solvent B CH_3CN, initial elution with A for 20 min, then a linear gradient of B, 0−40% over 20 min and 40% B for 30 min.

5-[^{125}I]Iodo-3′-*O*-(17β-succinyl-5α-androstan-3-one)-*O*,*O*′-(di-*tert*-butyl)-2′-deoxyuridin-5′-yl Monophosphate (12). Method I. General procedure B was used. The radioiododestannylation mixture of **10** (120 μg) and [^{125}I]NaI (12 mCi) was purified by HPLC using the C18 column (720 μL injection volume), eluent, solvent A 50% CH_3CN, solvent B CH_3CN, all with 0.07% TFA, a linear gradient of B, 0−95% over 35 min, 95% B for 30 min. The main radioactive peak of **12** (10.23 mCi, 85%) was eluted from HPLC in three fractions within 22−24 min after the injection and was collected in 2.4 mL of the eluant. The excess of unreacted precursor **10** eluted from the column 23 min later (t_R = 47 min), allowing for a clean separation of **12**. Fractions 4−6 contained inorganic iodide (630 μCi, ∼5%). In fractions 16 and 17, a partially hydrolyzed product, phosphodiester of **12** (180 μCi, 1.5%), was detected. Analytical HPLC analyses (12 μCi **12** injected): t_R = 21.6 min (≥97% pure, Bioscan).

Method II. General procedure B was used. Compound **11** (120 μg) was reacted with [^{125}I]NaI (1−10 mCi). The reaction mixtures were purified on a C18 HPLC column (250−500 μL injection volume); eluent, solvent A H_2O, solvent B CH_3CN, both with 0.07% TFA, a linear gradient of B, 0−95% over 30 min, 95% B for 30 min. The radioactivity peak of **12** (88% average yield based on eight radioiododestannylations) was eluted in two fractions 37−38 min after injection (collected in 1.6 mL of the eluant). **12** was cleanly separated from the excess of unreacted precursor **11**, which eluted ∼3.5 min later (t_R = 41.3 min). Analytical HPLC analyses (8 μCi **12** injected): t_R = 37.4 min (≥98% pure, Bioscan).

5-[^{125}I]Iodo-3′-*O*-(17β-succinyl-5α-androstan-3-one)-2′-deoxyuridin-5′-yl Monophosphate (13). Into a glass tube containing di-*tert*-butyl phosphotriester **12**, purified as described above (1−10 mCi, dried residue collected after the HPLC separation), anhydrous CH_3CN (250 μL) was added and evaporated to

dryness with a stream of dry nitrogen. This evaporation was repeated three times, and the tube with **12** was kept under a high vacuum for 15 min. Anhydrous CH_3CN (200 μL) followed by TFA (30 μL) was added under nitrogen, and the reaction tube was tightly covered. Aliquots (0.5−1 μL) were taken periodically from the reaction mixture, and the progress of hydrolysis was monitored by HPLC: C18 column, eluent, solvent A H_2O, solvent B CH_3CN, all with 0.07% TFA, a linear gradient of B, 0−95% over 30 min, then 95% B for 30 min. After 15 min of hydrolysis, three radioactive products were detected: t_R = 37.4 min (32%), t_R = 32.7 min (53%), and t_R = 29.5 min (15%), corresponding to starting di-*tert*-butyl phosphotriester **12**, partially hydrolyzed **12** (mono-*tert*-butyl phosphodiester), and phosphate **13**. The reaction was completed within 45−60 min, and HPLC analyses showed two products: 94% **13** with t_R = 29.5 min and ∼6% of mono-*tert*-butyl phosphodiester with t_R = 32.7 min. The crude reaction mixture was neutralized with a solution of 1.0 N NaOH (∼330 μL). Excess acetonitrile was partially evaporated with a stream of nitrogen, and the entire mixture (500 μL) was injected and purified by HPLC: C18 column, eluent, solvent A potassium phosphate buffered saline (0.05 M PBS, pH 7.1), solvent B CH_3CN, a linear gradient of B, 0−50% over 30 min, then 50% B for 30 min. The main radioactive peak was **13**, which eluted in three fractions (34−36 min) after the injection and was collected in a volume of 2.5 mL. The average radiochemical yield was 91% as calculated from nine independently performed hydrolyses. Analytical HPLC (5 μCi **13** injected): t_R = 35 min (≥97% pure, Bioscan).

5-[^{125}I]Iodo-3′-*O*-succinyl-2′-deoxyuridine Ethyl Ester (17). General procedure B was used. The main radioactive peak from the reaction mixtures of **16** (100 μg) with [^{125}I]NaI/NaOH (1−5 mCi) was eluted from HPLC in two fractions within 23−24 min postinjection and was collected in a volume of 1.6 mL. The excess of unreacted precursor **16** was cleanly separated from **17** and eluted 29.6 min after the injection. The average radiochemical yield, calculated on the basis of the results of four radioiododestannylations, was 90%, and the product was 95% **17** with ∼5% inorganic iodide collected in four initial fractions 4−7 min after the injection. Analytical HPLC analyses (4 μCi **17** injected): t_R = 23.4 min (≥98% pure, Bioscan) on the C18 analytical column, eluent, solvent A 10% CH_3CN, solvent B CH_3CN, a linear gradient of B, 0−95% over 40 min, then 95% B for 20 min; t_R = 29.7 min (≥98% pure, Bioscan) on the C18 column, eluent, solvent A H_2O, solvent B CH_3CN, both solvents with 0.07% TFA, the initial elution with A for 10 min, then a linear gradient of B, 0−95% over 20 min and held at 95% B for 30 min.

5-[^{125}I]Iodo-*O*,*O*′-(di-*tert*-butyl)-2′-deoxyuridin-5′-yl Monophosphate (19). General Pprocedure B was used. The main radioactive peak was separated on HPLC using conditions developed for the analysis of compound **5**. Radioiodinated product **19** eluted in three fractions within 23−25 min after the injection of the quenched reaction mixture and was collected in a volume of 2.4 mL. Analytical HPLC analyses (1.8 μCi **19** injected): t_R = 25.7 min, eluent, as used during the separation. The excess of unreacted tin precursor **18** was well separated and eluted 29 min postinjection. The average radiochemical yield of **19** was 87%, as calculated from six conducted radioiododestannylations, and the product was 96% **19** with ∼4% inorganic iodide. Analytical HPLC analyses (5 μCi **19** injected): t_R = 30.4 min (≥98% pure, Bioscan) on the C18 analytical column, eluent, as for the analysis of **17**.

5-[^{125}I]Iodo-2′-deoxyuridine-5′-monophosphate (20). A sample of purified **19** (1−10 mCi), dried as described for **13**, was dissolved in anhydrous CH_3CN (200 μL), and 30 μL TFA was added. The reaction progress was monitored by HPLC: C18 column, eluent, solvent A H_2O, solvent B CH_3CN, all with 0.07% TFA, the initial elution with A (10 min) and a linear gradient of B, 0−95% over 20 min, then 95% B for 30 min. The reaction was completed within 35−45 min. The HPLC analysis showed a single main product of monophosphate **20** (t_R = 21.9 min, 95.7%) along with partially hydrolyzed mono-*tert*-butyl phosphodiester **19** (t_R = 26.1 min, ∼3%) and traces of **19** (t_R = 30.4 min, ∼1.5%). The reaction mixture was neutralized with 1.0 N NaOH (∼330 μL). Excess acetonitrile was evaporated with a stream of nitrogen and the mixture injected (∼500 μL) and purified by HPLC: C18 column, eluent, solvent A potassium phosphate buffered saline (0.05 M, pH 7.1), solvent B CH_3CN, the initial elution with 100% A (10 min) and a linear gradient of B, 0−50% over 20 min, then 50% B for 30 min. The radioactive peak was 90% **20** (average radiochemical yield calculated from five conducted hydrolyses) eluting in three fractions (10−13 min) after the injection and was collected in a volume of 2.5 mL. Analytical HPLC analyses (2.5 μCi **20** injected): t_R = 12.1 min (≥97% pure, Bioscan), eluent, as described above for the separation of **20**. Purified sample of **20** (7.5 μCi) was co-injected on the HPLC column with IUdR **1** (35 μg) (t_R = 26.7 min) and a commercial sample of 5-iodo-2′-deoxyuridine 5′-monophosphate (32 μg) (t_R = 11.9 min). A single radioactive peak eluted with t_R = 12 min, confirming the identity of radioiodinated product **20**.

Proteins, Sera, Buffers, and Cell Culture Reagents. Human SHBG (pure, lyophilized) was from Lee Biosolutions, Inc. (St. Louis, MO). RPMI-1640 medium, fetal bovine serum (FBS), L-glutamine, penicillin−streptomycin liquid, and sodium pyruvate were from GIBCO Invitrogen Cell Culture (Carlsbad, CA). Insulin and human, rabbit, and mouse serum were purchased from Sigma-Aldrich (St. Louis, MO). NE-PER nuclear and cytoplasmic extraction reagents were from Thermo Fisher Scientific (Rockford, IL). DNA extractor TIS kit was from WAKO (Wako Chemicals USA, Inc., Richmond, VA). CellTiter-Fluor cell viability assay or CellTiter 96 AQueous One Solution cell proliferation assay were used for the cell survival assessment (Promega Corporation, Madison, WI).

Cells. NIH:OVCAR-3 human ovarian epithelial adenocarcinoma cells, LNCaP human prostate carcinoma cells, PC-3 human prostate adenocarcinoma cells, and MCF7 mammary gland (breast) adenocarcinoma cells were purchased from American Type Culture Collection (ATCC; Manassas, VA). OVCAR-3 cells were grown in RPMI-1640 medium supplemented with 0.01 mg/mL bovine insulin, 2 mM L-glutamine, and FBS to a final concentration of 20%. When sufficient numbers of OVCAR-3 cells were produced, athymic NCr-nu/nu female mice were injected intraperitoneally (ip) with OVCAR-3 cells suspended in 0.4 mL of serum-free RPMI-1640 medium, and further propagation of these cells was from the ip xenografts. When the abdominal distention became apparent, mice were killed and the peritoneal cavity was lavaged with 2 mL of sterile PBS to recover nonadherent OVCAR-3 cells. Cells were centrifuged, the supernatant was discarded, and the cell pellet was resuspended in complete growth medium (95%) and DMSO (5%). Cells were stored in liquid N_2 until ready for use. LNCaP (low passage, < 25) were grown in RPMI-1640 containing 10% FBS, 100 μM sodium pyruvate, 10 mM HEPES, 0.15% sodium bicarbonate, and 0.45% glucose. PC-3 cells were also cultured in RPMI-1640 containing 10% FBS supplemented with 100 μM sodium pyruvate. MCF7 cells were grown in Eagle's minimum essential medium (ATCC) supplemented with 0.01 mg/mL bovine insulin and 10% FBS. All cell culture media were also supplemented with penicillin (100 U/mL) and streptomycin (100 μg/mL).

Stability in PBS and Cell Culture Media. Solutions of **8**, **13**, **17**, and **20** (∼0.85 μCi/μL) were incubated (up to 24 h) in PBS (50 mM phosphate, pH 7.2)/CH_3CN mixture (10:1, v/v, final pH 7.1) at ambient temperature. Samples (100 μL) were taken up periodically, acidified with 0.1 N HCl (10 μL), and 5 μL aliquots (∼4.5 μCi) were injected and analyzed on the HPLC system (Bioscan detector). Solutions of radioiodinated target compounds (**8**, **13**, **17**, **20**) in CH_3CN (5 μL, 9−12 μCi) were added to RPMI-1640 cell culture medium (960 μL), and CH_3CN (35 μL) was added. The resulting mixture was incubated at

ambient temperature. At each time point, 200 μL samples were taken up, CH_3CN (250 μL) was added, and samples were acidified with 0.1 N HCl (50 μL). Aliquots were centrifuged (2000 rpm, 15 min), and the volume of supernatants (400 μL) was reduced to ~50 μL with a stream of nitrogen. The resulting samples (pH 2−4), diluted with water (200 μL) and CH_3CN (30 μL), were injected (250 μL, ~1.3 μCi) and analyzed by HPLC.

Evaluation of Binding to SHBG and Serum Using HPLC. Binding properties of **8**, **13**, **17**, and **20** to purified human SHBG and to rabbit, mouse, and human serum were evaluated. Experiments to determine binding and stability were conducted as follows: into a 1.96 mL solution of tested serum diluted in PBS (1:1, v/v, pH 7.1) or into a PBS solution of SHBG (with and without albumin), ~20 μCi aliquot of the radioiodinated **8**, **13**, **17**, or **20** in 40 μL of CH_3CN was added. The resulting mixtures were briefly vortexed and incubated up to 24 h at ambient temperature. At selected times, a 0.5 mL volume (~5 μCi) was withdrawn and size exclusion HPLC analysis was performed on a TosoHaas TSK-GEL G3000SW (300 mm × 7.5 mm) column equipped with a TSK-SW guard column. Solvents were as follows: solvent A, 0.1 M potassium phosphate buffer (PB) and 0.1 M Na_2SO_4 mixed at 1:1 ratio [v/v], pH 6.8; solvent B, CH_3CN. The initial elution was with A for 20 min followed by a linear gradient of B 0−40% over 20 min, and 40% B was held for 30 min. Flow rate was 0.7 mL/min with the radioactivity and UV at 280 nm detection. In parallel to the size exclusion analyses, a second 1 mL aliquot was withdrawn from each tested mixture at the same time, and this was treated with 1 mL of CH_3CN to denature and precipitate proteins. These mixtures were vortexed briefly and centrifuged at 2000 rpm for 15 min. The radioactive supernatant (9−12 μCi) was removed, and 0.4 mL aliquots of supernatants were acidified to pH ~4 with 0.1 N HCl (15−20 μL). The excess of CH_3CN was evaporated with a stream of nitrogen. An amount of 100 μL of water was added, and a 100 μL sample (1.3−1.5 μCi) of the resulting clear solution was injected on the second HPLC system equipped with a reverse phase column (ACE C18, 5 μm, 4.6 mm × 250 mm). The elution for **8**, **13**, and **17** was at a rate of 0.8 mL/min with solvent A, H_2O, and solvent B, CH_3CN. Both solvents contained 0.07% TFA. The initial elution was with 100% A for 10 min, then a linear gradient of B from 0% to 95% over 30 min, and the solvent was held at 95% B for 20 min. HPLC analyses of mixtures containing **20** were done with solvent A, potassium phosphate buffered saline (0.05 M, pH 7.1), and solvent B, CH_3CN, with the initial elution using 100% A for 10 min followed by a linear gradient of B from 0% to 50% over 20 min and held at 50% B for 20 min. Only radioactivity was detected.

Evaluation of Binding to SHBG and Serum Using ITLC. 8 was dissolved in 0.1 M sodium phosphate/0.1 M sodium sulfate, pH 6.8, containing 25% CH_3CN at a concentration of 48 μCi/mL. Lyophilized human SHBG was reconstituted at 1 mg/mL in PBS containing 0.1% bovine serum albumin (BSA). The binding was evaluated at SHBG concentrations of 0, 0.07, and 0.14 mg/mL using ~10000 cpm **8**/μL of the incubation mixture. Sera were diluted at 1:5 (v/v) with PBS, and **8**, also at 10 000 cpm/μL of the incubation mixture, was added as described for SHBG. Mixtures were incubated for 1, 2, and 18 h. Aliquots were analyzed on ITLC using ethanol/PBS (1:9, v/v) as the solvent. When binding to serum from various species was analyzed, all samples for a given time were run simultaneously on the same 5 cm wide ITLC plate. Eluted plates were cut and slices counted in a γ-counter. Some plates were also placed on a Kodak XAR2 imaging film (Eastman Kodak Company, Rochester, NY). The exposed films were developed to visualize the radioactivity associated with each band.

Stability, Concentration- and Time-Dependent Uptake, and Subcellular Distribution of 8 in NIH:OVCAR-3 Cells. Cells taken from liquid N_2 storage were thawed rapidly in a 37 °C water bath and transferred into complete growth medium. The suspension was centrifuged for 10 min at 500 rpm. The cell pellet was resuspended in complete growth medium with charcoal−dextran-stripped FBS. Cell viability was determined using the Trypan blue method.[90] Cells were diluted to 5×10^7 viable cells/mL medium. Compound **8** dissolved in ethanol at 2 μCi/mL was added to the cell suspension to produce a final concentration of 0.1 μCi/mL. Two controls were prepared. The purpose of the first control, which contained only **8** in full cell culture medium, was to follow the stability of **8** in the absence of cells. The second comprised cells, which were given only 0.05 mL of ethanol, to measure if any changes in the cell viability were observed that did not depend on the uptake of the radioactive drug. All samples were incubated at 37 °C in an atmosphere of 5% CO_2 on a shaker. Aliquots of growth medium were withdrawn from tubes after 0, 15, 30, 60, 120, 180, and 240 min of incubation with cells and analyzed on silica gel TLC plates alongside the corresponding drug standard using 3:1 (v/v) mixture of ethyl acetate and hexane as the eluting solvent for **8**. Plates were analyzed either in a γ counter or via autoradiography. Percent recovered intact drug was calculated by normalizing the amount of the intact radioactive drug in cell-containing medium to the amount of drug incubated in medium only. After the last time point, the viability of cells in all tubes was determined.

For the uptake and subcellular distribution studies, OVCAR-3 cells were plated at 1×10^5 cells/well in six-well plates at least 72 h in advance and allowed to grow until ~30% confluent, at which time spent medium was discarded and replaced with fresh complete RPMI-1640 medium. Solutions of **8** in ethanol were prepared at 10 μCi/mL and added to cells to produce final concentrations ranging from 0.1 to 1.0 μCi/mL. Total volume of ethanol added to each well was 0.05 mL. Control cells were treated with ethanol only. After 6 h of incubation, radioactive medium was removed and reserved for the analyses of radioactivity. Cell monolayers were washed once, fresh complete medium was added, and plates were returned to the incubator for an additional 24 h. Cells were harvested, medium was collected, and cell pellets were processed using either NE-PER nuclear and cytoplasmic extraction kit or the Wako DNA extractor kit to determine the intracellular distribution of radioactivity or DNA-associated radioactivity, respectively. The OD260/280 ratio was used to determine DNA purity and concentration.[91] Values of > 1.7 were accepted.

Concentration- and Time-Dependent Uptake and Subcellular Distribution of 13 in NIH:OVCAR-3 Cells. Cells prepared as indicated above were treated with **13** at a concentration of 2.5 μCi/mL for 1, 3, 6, and 24 h at 37 °C in an atmosphere of 5% CO_2 on a shaker. At indicated times, cells were briefly centrifuged to produce a loose cell pellet, washed once with fresh complete medium, plated in T25 flasks, and incubated for 24, 48, and 120 h. The viability of cells was determined. At indicated times, cells were harvested and the uptake and subcellular distribution of ^{125}I were measured as described for **8**. For the concentration-dependent uptake, OVCAR-3 cells were plated at 1×10^5 cells/well in six-well plates at least 72 h in advance and allowed to grow until ~30% confluent, at which time the cultured medium was discarded and replaced with fresh complete RPMI-1640 medium. Solutions of **13** in ethanol were prepared at 10 μCi/mL and added to cells to produce final concentrations ranging from 0.1 to 1.0 μCi/mL. Total volume of ethanol added to each well was 0.05 mL. Control cells were treated with ethanol only. After 24 h of incubation, radioactive medium was removed and reserved for the analyses of radioactivity. Cell monolayers were washed once, fresh complete medium was added, and plates were returned to the incubator for an additional 24 h. Cells were harvested and processed as described above for **8**.

Concentration- and Time-Dependent Uptake and Subcellular Distribution of 13 in LNCaP Cells. All studies were conducted as described above for OVCAR-3 cells with the following

modifications: LNCaP cells were plated at 1×10^6 cells/well in six-well plates 48 h before the uptake study. Radioactive drug was added in charcoal-stripped medium, and cells were allowed to grow for up to 120 h. The subcellular localization of the radioactivity was also determined using 0.1 M citric acid to isolate pure nuclei pellets,[92] and their radioactive content was analyzed in a γ-counter. Cells were kept in citrate for 10−15 min with constant shaking to facilitate membrane disruption. Detached nuclei were collected into a test tube and centrifuged at 225 rpm for 10 min. Nuclei were enumerated with the aid of Trypan blue. Cells were also harvested from the identical set of plates using trypsin to measure total cellular uptake of radioactivity. Cell pellets were collected, and washed with PBS, cell viability was determined, and pellets were counted in a γ-counter.

Uptake in MCF7, PC-3, and LNCaP Cells in Cell Suspension. These cell lines were propagated as a monolayer. Twenty-four hours before the experiment, cells were harvested and subcultured into 75 cm^2 BD Falcon plastic flasks (BD, Franklin Lakes, NJ) at 1×10^5 cells/mL complete medium, appropriate for a given cell line as indicated above. When the cells reached ~70% confluency, full growth medium was replaced with serum-free medium for a period of 24 h. Cells were harvested and counted, their viability was determined, and the cells were aliquoted into test tubes at 1×10^6 cells per tube. Each experiment was run in triplicate. One set of cells received serum-free medium only to assess total binding of the radioactive drugs. The second set of tubes had serum-free medium supplemented with 100 nM DHT to compete binding of radioactive drugs. All cells were incubated in suspension for 24 h and centrifuged briefly at 1000 rpm. Media were removed from all tubes and replaced with 40 mM HEPES, pH 7.4, containing 0.1% bovine serum albumin (HEPES/BSA). Cell pellets were washed with HEPES/BSA. Identical volumes of **8** dissolved in HEPES/BSA at 0.3−3.0 μCi/mL were added to all tubes, and cells were incubated with **8** from 5 to 16 h at 4 °C to prevent cell proliferation and reuptake of **1** released from **8**. Medium was removed at the selected times, and 1 mL aliquots were counted in a γ-counter to determine the recovery of radioactivity after incubation and to assess the amount of nonspecific binding to tubes. Cells were washed at least twice with ice-cold PBS containing 0.1% BSA. Washes were combined, their volume was measured, and a 1 mL aliquot was counted in a γ-counter. After the last PBS wash, the supernatant was decanted and saved. Cell pellets were frozen and thawed, dissolved in 1 M NaOH, and counted in a γ-counter.

Uptake of 13 in Cells Grown in Monolayer. LNCaP cells were plated in a six-well plate at 1×10^6 cells per well in 5 mL of RPMI-1640 medium stripped with dextran-coated charcoal and allowed to attach overnight. Triplicate cells were incubated for 3 h with 1 μM DHT in ethanol (final concentration of ethanol of < 1.5%). The remaining wells were given identical volumes of ethanol. After 3 h at 37 °C, phosphate **13**, dissolved in ethanol, was added to all wells. Aliquots (100 μL) were withdrawn from wells to determine the added radioactivity in each well. Cells were grown in the presence of drugs for 24, 48, and 72 h, at which time the radioactive medium was replaced with fresh complete RPMI-1640 medium. Cells were either immediately trypsinized, counted, and their radioactive content determined in a γ-counter or allowed to continue to grow for 24, 48, and 72 h in fresh nonradioactive medium.

Cell Survival Studies. NIH:OVCAR-3 cells were plated in two 96-well plates at 4000 cells/well and allowed to attach for 48 h. Fresh complete medium supplemented with 20% charcoal−dextran-stripped FBS and containing various concentrations of radioactive drugs was added so that each concentration was tested in 12 wells. Cells were incubated with the radioactive drug for 6 h for **8** and 24 h for **13**. After removal of the radioactive medium, cells were given fresh medium and incubated for an additional 24 and 48 h. The cell survival was measured using either CellTiter-Fluor cell viability assay or CellTiter 96 AQueous One Solution cell proliferation assay. LNCaP cells were plated at 2000 cells/well and allowed to attach for 24 h, after which time all cell were given fresh, charcoal−dextran-stripped medium.

Mice. Female athymic NCr-nu/nu mice were from the National Cancer Institute at Frederick (Frederick, MD) or from Charles River (Wilmington, MA). Mice were allowed to acclimate for no less than 4 days after arrival to the UNMC facilities. All protocols involving mice were approved by the UNMC Institutional Animal Care and Use Committee. NIH:OVCAR-3 tumors were grown as the intraperitoneal xenografts. Mice were maintained on a normal diet. At 3 days before therapy experiments and up to 7 days after the last dose of the radioiodinated drug, drinking water was replaced daily with fresh 0.01% solution of potassium iodide prepared from the pharmaceutical grade supersaturated potassium iodide in distilled water (SSKI; potassium iodide oral solution, USP, Upsher-Smith Laboratories, Inc., Minneapolis, MN).

Biodistribution. NIH:OVCAR-3 cells propagated in vivo and recovered from ascites were resuspended in serum-free RPMI-1640 medium or physiological saline and implanted ip. Tumors were allowed to develop for up to 6 weeks. Drug **8** was administered ip in 0.4 mL of physiologic saline containing 0.1% albumin. An average dose of 1.12 (0.04) μCi/mouse was injected. Full syringes containing the dose and syringes after administration were weighed on an analytical balance to determine the weight of the dose injected into each mouse. Aliquots equivalent to 1 μL of the injected dose were counted in a γ-counter. Mice were killed at 1.5, 24, 48, and 72 h postinjection. Postmortem examination included the lavage of peritoneal cavity with 2 × 2 mL physiologic saline. Normal tissues and solid tumor deposits were harvested, and rinsed in saline and their wet weight and radioactive contents were determined. The peritoneal lavage samples were centrifugation at 1000 rpm for 10 min at 4 °C. Supernatants were removed, and radioactivity was determined. Tumor cell pellets were resuspended in 1 mL of PBS and counted in a γ-counter. Cells were suspended and washed twice with 5% perchloric acid for DNA precipitation. Acid washes and DNA pellets were counted in a γ-counter. Tissue uptake was calculated as percent injected dose per gram of tissue and as the tissue-to-blood ratio (radiolocalization index).

Therapy. Female athymic mice received intraperitoneal implant of 1.34×10^8 OVCAR-3 cells/mouse. Mice were randomly assigned to control and experimental groups. Control mice were either injected with PBS only or given ip injections of the nonradioactive analogue **6**. The experimental group was treated ip with **8**. The experimental design also included one control group, which did not have tumors but was treated with the radioactive drug to determine the effects of the ip injected radioactivity. For drug **8**, three treatment schemes were followed.

Experiment I. In the first set of experiments, 12 days after tumor implantation, mice were given a single ip dose of **8**. On average 14 μCi **8**/mouse in 0.5 mL of physiologic saline containing 1% albumin and 0.01% ethanol (v/v), to prevent the precipitation of the drug from the solution, was injected. Control mice were injected with **6** in the same vehicle. Body weight of all mice was determined every 2−3 days until the termination of the study. Five weeks after tumor implantation, mice were euthanized according to the AVMA guidelines, the necropsy was performed, whole body radioactivity was determined, and biodistribution was conducted. The peritoneal cavity was lavaged with 2 mL of PBS to recover nonadherent OVCAR-3 cells and ascites. Cell viability and radioactive content of the nonadherent cancer cells were determined, including the DNA bound iodine-125. Solid tumors were dissected, and their weight and radioactivity were measured. Several normal tissues and blood were also harvested, and their radioactive content was determined. Blood was collected via cardiac puncture. Hematocrit was determined by standard techniques. HemoCue was used

to measure hemoglobin levels (Angelholm, Sweden). Tissues were dissected and rinsed in PBS, and their wet weight was determined. Dissected tissues were placed in γ-counter tubes, and their radioactive content was measured.

Experiment II. Twelve days after ip injection of OVCAR-3 cells, mice were randomly separated into two groups: control mice receiving only 0.5 mL of vehicle ip and experimental mice receiving **8** in the same vehicle. The administration of **8** was in three escalating doses injected ip as follows: day 1, 5 μCi **8**/mouse; day 2, 10 μCi **8**/mouse; day 3, 15 μCi **8**/mouse. Mice in the experimental group received on average 30 μCi **8**/mouse. Five weeks after the tumor implantation, mice were euthanized and the necropsy was performed as described above.

Experiment III. In this group, the drug treatment was started 9 days after the OVCAR-3 cells ip implant. Mice were randomly assigned into two groups: the experimental group treated with six fractionated doses of **8** every 4 days for the total dose of 185 μCi **8**/mouse; control group of mice treated with vehicle only. Two weeks after the last dose of **8**, mice were euthanized and the necropsy was conducted as describe above.

Experiment IV. All therapy studies with drug **13** were conducted in mice bearing established, 31-day old ip xenografts of OVCAR-3. The drug **13**, 250 μCi/mouse, one ip dose, was coinjected with 10 μg of SHBG in 0.4 mL of PBS. One group of control mice received SHBG only in 0.4 mL of PBS, the second PBS alone. The study was terminated after 24 days because several SHBG-treated mice developed massive peritoneal ascites. The necropsy protocol described above was followed.

Experiment V. Compound **13** was also used in the fractionated therapy regimen in mice bearing OVCAR-3 ip xenografts. This study was conducted similarly to experiment III described above. The drug **13** was administered in fractionated doses (average 39.50 μCi/dose/mouse). One group of OVCAR-3-bearing control mice received six sham injections of 0.4 mL of PBS. The second control group included healthy mice (i.e., no OVCAR-3 implant). These mice were treated with **13** using the same schedule to compare normal tissue retention and distribution of **13**. The necropsy protocol described above was followed. Cancer cells recovered with saline lavage were subjected to trichloroacetic acid (TCA) precipitation to determine the DNA-associated radioactivity. First, OVCAR-3 cells were counted and their viability was determined using the Trypan blue assay. The cell pellet was washed with ice-cold saline to determine the unbound radioactivity. A fresh aliquot of saline was added to reconstitute all cancer cell pellets at the same concentration of 1×10^7 cells/mL. Mixtures were vortexed to produce cell suspension. Then 1 mL of suspension was removed for radioactivity determination. Two 1 mL samples were removed for DNA analyses. Cells were centrifuged, the supernatant was taken for radioactivity counting, and the ice-cold pellet was treated with 1.5 mL of ice-cold 10% TCA at 4 °C overnight to precipitate DNA. Tubes containing DNA pellets were centrifuged. DNA was washed twice with ice-cold 10% TCA, and all fractions including the DNA pellet were counted in a γ-counter.

Statistical Analyses. Summary statistics were performed using a two-sided, unpaired Student's t test with a significance level of $P = 0.05$. Therapy data were evaluated using one-way analysis of variance with Tukey−Kramer or Dunnett multiple comparison tests using SigmaPlot/SigmaStat (Systat Software, Inc., Richmond, CA) and GraphPad InStat computer software (GraphPad Software, Inc., La Jolla, CA).

Acknowledgment. This work was supported by the U.S. Department of Defense Congressionally Directed Medical Research Programs (Grants W81XWH-04-1-0463 and DAMD17-99-1-9313 to J.B.-K.). Mass spectrometry analyses were provided by the Washington University Mass Spectrometry Resource with support from the NIH/National Center for Research Resources (Grant 2P41RR000954) and the Mass Spectrometry Center, University of Nebraska, Lincoln, NE. Nuclear Magnetic Resonance analyses were conducted at the UNMC Eppley Institute NMR Facility managed by E. L. Ezell. The modeling was performed by Dr. Leo Kinarsky, Director of the Molecular Modeling Facility, Eppley Institute for Research in Cancer and Allied Diseases, UNMC. The authors thank S. Franks, K. Vang, and N. J. Wicker for their technical assistance. The authors also acknowledge the participation of the UNMC SURP students A. Augustine and J. McGarry, whose efforts were supported by a fellowship funded by the Society of Nuclear Medicine.

Supporting Information Available: Preparative and analytical HPLC data, binding, stability studies, in vivo localization indices, control body weights, and molecular docking. This material is available free of charge via the Internet at http://pubs.acs.org.

References

(1) Schippinger, W.; Regitnig, P.; Dandachi, N.; Wernecke, K. D.; Bauernhofer, T.; Samonigg, H.; Moinfar, F. Evaluation of the prognostic significance of androgen receptor expression in metastatic breast cancer. *Virchows Arch*. **2006**, *449*, 24–30.
(2) Agrawal, A. K.; Jeleń, M.; Grzebieniak, Z.; Zukrowski, P.; Rudnicki, J.; Nienartowicz, E. Androgen receptors as a prognostic and predictive factor in breast cancer. *Folia Histochem. Cytobiol*. **2008**, *46*, 269–276.
(3) Ogawa, Y.; Hai, E.; Matsumoto, K.; Ikeda, K.; Tokunaga, S.; Nagahara, H.; Sakurai, K.; Inoue, T.; Nishiguchi, Y. Androgen receptor expression in breast cancer: relationship with clinicopathological factors and biomarkers. *Int. J. Clin. Oncol*. **2008**, *13*, 431–435.
(4) Agoff, S. N.; Swanson, P. E.; Linden, H.; Hawes, S. E.; Lawton, T. J. Androgen receptor expression in estrogen receptor-negative breast cancer. Immunohistochemical, clinical, and prognostic associations. *Am. J. Clin. Pathol*. **2003**, *120*, 725–731.
(5) Culig, Z.; Klocker, H.; Bartsch, G.; Steiner, H.; Hobisch, A. Androgen receptors in prostate cancer. *J. Urol*. **2003**, *170*, 1363–1369.
(6) Taplin, M. E.; Balk, S. P. Androgen receptor: a key molecule in the progression of prostate cancer to hormone independence. *J. Cell. Biochem*. **2004**, *91*, 483–490.
(7) Chodak, G. W.; Kranc, D. M.; Puy, L. A.; Takeda, H.; Johnson, K.; Chang, C. Nuclear localization of androgen receptor in heterogeneous samples of normal, hyperplastic and neoplastic human prostate. *J. Urol*. **1992**, *147*, 798–803.
(8) Donovan, M. J.; Hamann, S.; Clayton, M.; Khan, F. M.; Sapir, M.; Bayer-Zubek, V.; Fernandez, G.; Mesa-Tejada, R.; Teverovskiy, M.; Reuter, V. E.; Scardino, P. T.; Cordon-Cardo, C. Systems pathology approach for the prediction of prostate cancer progression after radical prostatectomy. *J. Clin. Oncol*. **2008**, *26*, 3923–3929.
(9) Palmberg, C.; Koivisto, P.; Kakkola, L.; Tammela, T. L.; Kallioniemi, O. P.; Visakorpi, T. Androgen receptor gene amplification at primary progression predicts response to combined androgen blockade as second line therapy for advanced prostate cancer. *J. Urol*. **2000**, *164*, 1992–1995.
(10) Chen, Y.; Sawyers, C. L.; Scher, H. I. Targeting the androgen receptor pathway in prostate cancer. *Curr. Opin. Pharmacol*. **2008**, *8*, 440–448.
(11) Kominea, A.; Konstantinopoulos, P. A.; Kapranos, N.; Vandoros, G.; Gkermpesi, M.; Andricopoulos, P.; Artelaris, S.; Savva, S.; Varakis, I.; Sotiropoulou-Bonikou, G.; Papavassiliou, A. G. Androgen receptor (AR) expression is an independent unfavorable prognostic factor in gastric cancer. *J. Cancer. Res. Clin. Oncol*. **2004**, *130*, 253–258.
(12) Kuhnel, R.; de Graaff, J.; Rao, B. R.; Stolk, J. G. Androgen receptor predominance in human ovarian carcinoma. *J. Steroid. Biochem*. **1987**, *26*, 393–397.
(13) Risch, H. A. Hormonal etiology of epithelial ovarian cancer, with a hypothesis concerning the role of androgens and progesterone. *J. Natl. Cancer Inst*. **1998**, *90*, 1774–1786.
(14) Scambia, G.; Benedetti Panici, P.; Ferrandina, G.; Battaglia, F.; Baiocchi, G.; Di Stefano, P.; Tinari, N.; Coronetta, F.; Piantelli, M.; Natali, P.; Iacobelli, S.; Mancuso, S. Expression of HER-2/neu

oncoprotein, DNA-ploidy and S-phase fraction in advanced ovarian cancer. *Int. J. Gynecol. Cancer* **1993**, *3*, 271–278.
(15) Chadha, S.; Rao, B. R.; Slotman, B. J.; van Vroonhoven, C. C.; van der Kwast, T. H. An immunohistochemical evaluation of androgen and progesterone receptors in ovarian tumors. *Hum. Pathol*. **1993**, *24*, 90–95.
(16) Poisson, M.; Pertuiset, B. F.; Hauw, J. J.; Philippon, J.; Buge, A.; Moguilewsky, M.; Philibert, D. Steroid hormone receptors in human meningiomas, gliomas and brain metastases. *J. Neurooncol*. **1983**, *1*, 179–189.
(17) Boix, L.; Bruix, J.; Castells, A.; Fuster, J.; Bru, C.; Visa, J.; Rivera, F.; Rodes, J. Sex hormone receptors in hepatocellular carcinoma. Is there a rationale for hormonal treatment? *J. Hepatol*. **1993**, *17*, 187–191.
(18) Beattie, C. W.; Hansen, N. W.; Thomas, P. A. Steroid receptors in human lung cancer. *Cancer Res*. **1985**, *45*, 4206–4214.
(19) Kaiser, U.; Hofmann, J.; Schilli, M.; Wegmann, B.; Klotz, U.; Wedel, S.; Virmani, A. K.; Wollmer, E.; Branscheid, D.; Gazdar, A. F.; Havemann, K. Steroid-hormone receptors in cell lines and tumor biopsies of human lung cancer. *Int. J. Cancer* **1996**, *67*, 357–364.
(20) Ito, K.; Suzuki, T.; Akahira, J.; Moriya, T.; Kaneko, C.; Utsunomiya, H.; Yaegashi, N.; Okamura, K.; Sasano, H. Expression of androgen receptor and 5alpha-reductases in the human normal endometrium and its disorders. *Int. J. Cancer*. **2002**, *99*, 652–657.
(21) Nahleh, Z. Androgen receptor as a target for the treatment of hormone receptor-negative breast cancer: an unchartered territory. *Future Oncol*. **2008**, *4*, 15–21.
(22) Olsen, C. M.; Green, A. C.; Nagle, C. M.; Jordan, S. J.; Whiteman, D. C.; Bain, C. J.; Webb, P. M. Australian Cancer Study Group (Ovarian Cancer) and the Australian Ovarian Cancer Study Group. Epithelial ovarian cancer: testing the "androgens hypothesis". *Endocr.-Relat. Cancer* **2008**, *15*, 1061–1068.
(23) Tworoger, S. S.; Lee, I. M.; Buring, J. E.; Hankinson, S. E. Plasma androgen concentrations and risk of incident ovarian cancer. *Am. J. Epidemiol*. **2008**, *167*, 211–218.
(24) Vassilomanolakis, M.; Koumakis, G.; Barbounis, V.; Hajichristou, H.; Tsousis, S.; Efremidis, A. A phase II study of flutamide in ovarian cancer. *Oncology* **1997**, *54*, 199–202.
(25) Tumolo, S.; Rao, B. R.; van der Burg, M. E.; Guastalla, J. P.; Renard, J.; Vermorken, J. B. Phase II trial of flutamide in advanced ovarian cancer: an EORTC Gynaecological Cancer Cooperative Group study. *Eur. J. Cancer* **1994**, *30A*, 911–914.
(26) Risch, H. A. Hormonal etiology of epithelial ovarian cancer, with a hypothesis concerning the role of androgens and progesterone. *J. Natl. Cancer Inst*. **1998**, *90*, 1774–1786.
(27) Kolfschoten, G. M.; Hulscher, T. M.; Pinedo, H. M.; Boven, E. Drug resistance features and S-phase fraction as possible determinants for drug response in a panel of human ovarian cancer xenografts. *Br. J. Cancer*. **2000**, *83*, 921–917.
(28) Reles, A. E.; Gee, C.; Schellschmidt, I.; Schmider, A.; Unger, M.; Friedmann, W.; Lichtenegger, W.; Press, M. F. Prognostic significance of DNA content and S-phase fraction in epithelial ovarian carcinomas analyzed by image cytometry. *Gynecol. Oncol*. **1998**, *71*, 3–13.
(29) Kimball, R. E.; Schlaerth, J. B.; Kute, T. E.; Schlaerth, A. C.; Santoso, J.; Ballon, S. C.; Spirtos, N. M. Flow cytometric analysis of lymph node metastases in advanced ovarian cancer: clinical and biologic significance. *Am. J. Obstet. Gynecol*. **1997**, *176*, 1319–1326.
(30) Abdel-Wahab, M.; Krishan, A.; Milikowski, C.; Wahab, A. A.; Walker, G.; Markoe, A. Androgen receptor antigen density and S-phase fraction in prostate cancer: a pilot study. *Prostate Cancer Prostatic Dis*. **2003**, *6*, 294–300.
(31) Koivisto, P. Aneuploidy and rapid cell proliferation in recurrent prostate cancers with androgen receptor gene amplification. *Prostate Cancer Prostatic Dis*. **1997**, *1*, 21–25.
(32) Samoszuk, M. K.; Sallash, G.; Chen, K.; Carlton, E.; Oldaker, T. Association between flow cytometric S-phase fraction and apoptotic rate in breast cancer. *Cytometry* **1996**, *26*, 281–285.
(33) Largillier, R.; Namer, M.; Ramaioli, A.; Ferrero, J. M.; Magné, N.; Courdi, A.; Leblanc-Talent, P.; Formento, P.; Ettore, F.; Milano, G. Prognostic value of S-phase fraction in 920 breast cancer patients: focus on T1N0 status. *Int. J. Biol. Markers* **2003**, *18*, 273–279.
(34) Del Casar, J. M.; Martín, A.; García, C.; Corte, M. D.; Alvarez, A.; Junquera, S.; González, L. O.; Bongera, M.; García-Muñiz, J. L.; Allende, M. T.; Vizoso, F. Characterization of breast cancer subtypes by quantitative assessment of biological parameters: relationship with clinicopathological characteristics, biological features and prognosis. *Eur. J. Obstet. Gynecol. Reprod. Biol*. **2008**, *141*, 147–152.
(35) Kabalka, G. W.; Varma, R. S. The synthesis of radiolabelled compounds via organometalic intermediates. *Tetrahedron* **1989**, *45*, 6601–6621.
(36) Pereyre, M.; Quintard, J. P.; Rahm, A. *Tin in Organic Synthesis*; Butterworth-Heinemann: London, 1987; pp 136−140.
(37) Volovelskii, L. N.; Rastrepina, I. A.; Popova, N. V.; Koryukina, V. N.; Kustova, S. P. Acylation of steroidal alcohols by *N*-succinamic acids. *Khim. Prir. Soedin*. **1985**, *5*, 700–704.
(38) Van Boom, J.; Burgers, P. Use of levulinic acid in the protection of oligonucleotides via the modified phosphotriester method: synthesis of decarbonucleotide U-A-U-A-U-A-U-A-U-A. *Tetrahedron Lett*. **1976**, *21*, 4875–4878.
(39) Dougan, H.; Rennie, B. A.; Lyster, D. M.; Sacks, S. L. No-carrier-added [^{123}I]-1-(β-D-arabinofuranosyl)-5(*E*)-(2-iodovinyluracil (IVaraU): high yielding radiolabeling via organotin and exchange reactions. *Appl. Radiat. Isot*. **1994**, *45*, 795–801.
(40) Fraker, P. J.; Speck, J. C. Protein and cell membrane iodinations with a sparingly soluble chloroamide, 1,3,4,6-tetrachloro-3a, 6a-diphenylglycoluril. *Biochem. Biophys. Res. Commun*. **1978**, *80*, 849–857.
(41) Van Dort, M. E.; Hagen, C. A. Synthesis of (*E*)-4-[4,4-dimethyl-2,5-dioxo-3-{1′-(^{125}I)iodo-1″-propen-3″-yl}-1-imidazolidinyl]-2-trifluoromethylbenzonitrile: a potential radioligand for the androgen receptor. *J. Labelled Compd. Radiopharm*. **2001**, *44*, 47–54.
(42) Baldwin, R. M.; Zea-Ponce, Y.; Zoghbi, S. S.; Laurelle, M.; Al-Tikriti, M. S.; Sybirska, E. H.; Malison, R. T.; Neumeyer, J. L.; Milius, R. A. Evaluation of the monoamine uptake site ligand [^{123}I]methyl-3β(4-iodophenyl)tropane-2β-carboxylate ([^{123}I]-β-CIT) in nonhuman primates: pharmacokinetics, biodistribution and SPECT brain imaging co-registered with MRI. *Nucl. Med. Biol*. **1993**, *20*, 597–606.
(43) Baranowska-Kortylewicz, J.; Helseth, L. D.; Lai, J.; Schneiderman, M. H.; Schneiderman, G. S.; Dalrymple, G. V. Radiolabeling kit/generator for 5-radiohalogenated uridines. *J. Labelled Compd. Radiopharm*. **1994**, *34*, 513–521.
(44) Hamilton, T. C.; Young, R. C.; McKoy, W. M.; Grotzinger, K. R.; Green, J. A.; Chu, E. W.; Whang-Peng, J.; Rogan, A. M.; Green, W. R.; Ozols, R. F. Characterization of a human ovarian carcinoma cell line (NIH:OVCAR-3) with androgen and estrogen receptors. *Cancer Res*. **1983**, *43*, 5379–5389.
(45) Mitchell, S.; Abel, P.; Ware, M.; Stamp, G.; Lalani, E. Phenotypic and genotypic characterization of commonly used human prostatic cell lines. *BJU Int*. **2000**, *85*, 932–944.
(46) Evangelou, A.; Jindal, S. K.; Brown, T. J.; Letarte, M. Down-regulation of transforming growth factor beta receptors by androgen in ovarian cancer cells. *Cancer Res*. **2000**, *60*, 929–935.
(47) Andò, S.; De Amicis, F.; Rago, V.; Carpino, A.; Maggiolini, M.; Panno, M. L.; Lanzino, M. Breast cancer: from estrogen to androgen receptor. *Mol. Cell. Endocrinol*. **2002**, *193*, 121–128.
(48) Magklara, A.; Brown, T. J.; Diamandis, E. P. Characterization of androgen receptor and nuclear receptor co-regulator expression in human breast cancer cell lines exhibiting differential regulation of kallikreins 2 and 3. *Int. J. Cancer* **2002**, *100*, 507–514.
(49) Humm, J. L.; Howell, R. W.; Rao, D. V. Dosimetry of Auger-electron-emitting radionuclides: report no. 3 of AAPM Nuclear Medicine Task Group No. 6. *Med. Phys*. **1994**, *21*, 1901–1915.
(50) Turner, G. N.; Nobis, P.; Dewey, W. C. Fragmentation of chromatin with ^{125}I radioactive disintegrations. *Biophys. J*. **1976**, *16*, 1003–1012.
(51) Painter, R. B; Young, B. R; Burk, H. J. Non-repairable strand breaks induced by ^{125}I incorporated into mammalian DNA. *Proc. Natl. Acad. Sci. U.S.A*. **1974**, *71*, 4836–4838.
(52) Pastwa, E.; Neumann, R. D.; Mezhevaya, K.; Winters, T. A. Repair of radiation-induced DNA double-strand breaks is dependent upon radiation quality and the structural complexity of double-strand breaks. *Radiat. Res*. **2003**, *159*, 251–261.
(53) Hampton, A.; Hampton, E. G.; Eidinoff, M. L. Nucleotides. III. Synthesis and effects with cells in culture of 131-I-labeled 5-iodo-2'-deoxyuridine-5′-phosphate. *Biochem. Pharmacol*. **1962**, *11*, 155–159.
(54) Seitz, U.; Wagner, M.; Neumaier, B.; Wawra, E.; Glatting, G.; Leder, G.; Schmid, R. M.; Reske, S. N. Evaluation of pyrimidine metabolising enzymes and in vitro uptake of 3′-[(18)F]fluoro-3′-deoxythymidine ([(18)F]FLT) in pancreatic cancer cell lines. *Eur. J. Nucl. Med. Mol. Imaging* **2002**, *29*, 1174–1181.
(55) Aubé, M.; Larochelle, C.; Ayotte, P. 1,1-Dichloro-2,2-bis(*p*-chlorophenyl)ethylene (*p,p*′-DDE) disrupts the estrogen-androgen balance regulating the growth of hormone-dependent breast cancer cells. *Breast Cancer Res*. **2008**, *10*, R16.
(56) Katsuoka, Y.; Hoshino, H.; Shiramizu, M.; Sakabe, K.; Seiki, K. Autoradiographic and cytochemical localization of androgen in human prostatic cancer cell lines. *Urology* **1986**, *28*, 228–231.

(57) Tilley, W. D.; Wilson, C. M.; Marcelli, M.; McPhaul, M. J. Androgen receptor gene expression in human prostate carcinoma cell lines. *Cancer Res*. **1990**, *50*, 5382–5386.
(58) Hu, Y. C.; Wang, P. H.; Yeh, S.; Wang, R. S.; Xie, C.; Xu, Q.; Zhou, X.; Chao, H. T.; Tsai, M. Y.; Chang, C. Subfertility and defective folliculogenesis in female mice lacking androgen receptor. *Proc. Natl. Acad. Sci. U.S.A*. **2004**, *101*, 11209–11214.
(59) de Moor, P.; Verhoeven, G.; Heyns, W. A comparative study of the androgen receptor apparatus in adult rodents. *J. Steroid Biochem*. **1975**, *6*, 437–442.
(60) Pelletier, G.; Luu-The, V.; Li, S.; Labrie, F. Localization and estrogenic regulation of androgen receptor mRNA expression in the mouse uterus and vagina. *J. Endocrinol*. **2004**, *180*, 77–85.
(61) Baranowska-Kortylewicz, J.; Nearman, J.; Kortylewicz, Z. P. Effect of sex hormone binding globulin on the development of ovarian cancer in a mouse model. *Open Cancer J*. **2008**, *2*, 59–65.
(62) Lee, E. C.; Tenniswood, M. P. Emergence of metastatic hormone-refractory disease in prostate cancer after anti-androgen therapy. *J. Cell. Biochem*. **2004**, *91*, 662–670.
(63) Mohler, J. L. Castration-recurrent prostate cancer is not androgen-independent. *Adv. Exp. Med. Biol*. **2008**, *617*, 223–234.
(64) Gaston, K. E.; Kim, D.; Singh, S.; Ford, O. H.; Mohler, J. L. Racial differences in androgen receptor protein expression in men with clinically localized prostate cancer. *J. Urol*. **2003**, *170*, 990–993.
(65) Lange, E. M.; Sarma, A. V.; Ray, A.; Wang, Y.; Ho, L. A.; Anderson, S. A.; Cunningham, J. M.; Cooney, K. A. The androgen receptor CAG and GGN repeat polymorphisms and prostate cancer susceptibility in African-American men: results from the Flint Men's Health Study. *J. Hum. Genet*. **2008**, *53*, 220–226.
(66) Berger, G.; Maziere, M.; Prenant, C.; Sastre, J.; Comar, D. Synthesis of high specific activity 11C 17 alpha methyltestosterone. *Int. J. Appl. Radiat. Isot*. **1981**, *32*, 811–815.
(67) Liu, A.; Carlson, K. E.; Katzenellenbogen, J. A. Synthesis of high affinity fluorine-substituted ligands for the androgen receptor. Potential agents for imaging prostatic cancer by positron emission tomography. *J. Med. Chem*. **1992**, *35*, 2113–2129.
(68) Garg, P. K.; Labaree, D. C.; Hoyte, R. M.; Hochberg, R. B. [7alpha-^{18}F]fluoro-17alpha-methyl-5alpha-dihydrotestosterone: a ligand for androgen receptor-mediated imaging of prostate cancer. *Nucl. Med. Biol*. **2001**, *28*, 85–90.
(69) Ali, H.; Rousseau, J.; Ahmed, N.; Guertin, V.; Hochberg, R. B.; van Lier, J. E. Synthesis of the 7alpha-cyano-(17alpha,20*E*/*Z*)-[^{125}I]iodovinyl-19-nortestosterones: potential radioligands for androgen and progesterone receptors. *Steroids* **2003**, *68*, 1163–1171.
(70) Dehdashti, F.; Picus, J.; Michalski, J. M.; Dence, C. S.; Siegel, B. A.; Katzenellenbogen, J. A.; Welch, M. J. Positron tomographic assessment of androgen receptors in prostatic carcinoma. *Eur. J. Nucl. Med. Mol. Imaging* **2005**, *32*, 344–350.
(71) Parent, E. E.; Carlson, K. E.; Katzenellenbogen, J. A. Synthesis of 7alpha-(fluoromethyl)dihydrotestosterone and 7alpha-(fluoromethyl)nortestosterone, structurally paired androgens designed to probe the role of sex hormone binding globulin in imaging androgen receptors in prostate tumors by positron emission tomography. *J. Org. Chem*. **2007**, *72*, 5546–5554.
(72) He, H.; Morely, J. E.; Silva-Lopez, E.; Bottenus, B.; Montajano, M.; Fugate, G. A.; Twamley, B.; Benny, P. D. Synthesis and characterization of nonsteroidal-linked M(CO)(3)+ (M = ^{99m}Tc, Re) compounds based on the androgen receptor targeting molecule flutamide. *Bioconjugate Chem*. **2009**, *20*, 78–86.
(73) Nakhla, A. M.; Rosner, W. Stimulation of prostate cancer growth by androgens and estrogens through the intermediacy of sex hormone-binding globulin. *Endocrinology* **1996**, *137*, 4126–4129.
(74) Hryb, D. J.; Nakhla, A. M.; Kahn, S. M.; St George, J.; Levy, N. C.; Romas, N. A.; Rosner, W. Sex hormone-binding globulin in the human prostate is locally synthesized and may act as an autocrine/paracrine effector. *J. Biol. Chem*. **2002**, *277*, 26618–26622.
(75) Kahn, S. M.; Li, Y. H.; Hryb, D. J.; Nakhla, A. M.; Romas, N. A.; Cheong, J.; Rosner, W. Sex hormone-binding globulin influences gene expression of LNCaP and MCF-7 cells in response to androgen and estrogen treatment. *Adv. Exp. Med. Biol*. **2008**, *617*, 557–564.
(76) Hammes, A.; Andreassen, T. K.; Spoelgen, R.; Raila, J.; Hubner, N.; Schulz, H.; Metzger, J.; Schweigert, F. J.; Luppa, P. B.; Nykjaer, A.; Willnow, T. E. Role of endocytosis in cellular uptake of sex steroids. *Cell* **2005**, *122*, 751–762.
(77) Porto, C. S.; Gunsalus, G. L.; Bardin, C. W.; Phillips, D. M.; Musto, N. A. Receptor-mediated endocytosis of an extracellular steroid-binding protein (TeBG) in MCF-7 human breast cancer cells. *Endocrinology* **1991**, *129*, 436–445.
(78) Parent, E. E.; Dence, C. S.; Sharp, T. L.; Welch, M. J.; Katzenellenbogen, J. A. 7alpha-^{18}F-fluoromethyl-dihydrotestosterone and 7alpha-^{18}F-fluoromethyl-nortestosterone: ligands to determine the role of sex hormone-binding globulin for steroidal radiopharmaceuticals. *J. Nucl. Med*. **2008**, *49*, 987–994.
(79) Fortunati, N. Sex hormone-binding globulin: not only a transport protein. What news is around the corner? *J. Endocrinol. Invest*. **1999**, *22*, 223–234.
(80) Caldwell, J. D.; Shapiro, R. A.; Jirikowski, G. F.; Suleman, F. Internalization of sex hormone-binding globulin into neurons and brain cells in vitro and in vivo. *Neuroendocrinology* **2007**, *86*, 84–93.
(81) Hryb, D. J.; Khan, M. S.; Romas, N. A.; Rosner, W. The control of the interaction of sex hormone-binding globulin with its receptor by steroid hormones. *J. Biol. Chem*. **1990**, *265*, 6048–6054.
(82) Papadopoulou, N.; Papakonstanti, E. A.; Kallergi, G.; Alevizopoulos, K.; Stournaras, C. Membrane androgen receptor activation in prostate and breast tumor cells: molecular signaling and clinical impact. *IUBMB Life* **2009**, *61*, 56–61.
(83) Steinsapir, J.; Socci, R.; Reinach, P. Effects of androgen on intracellular calcium of LNCaP cells. *Biochem. Biophys. Res. Commun*. **1991**, *179*, 90–96.
(84) Hatzoglou, A.; Kampa, M.; Kogia, C.; Charalampopoulos, I.; Theodoropoulos, P. A.; Anezinis, P.; Dambaki, C.; Papakonstanti, E. A.; Stathopoulos, E. N.; Stournaras, C.; Gravanis, A.; Castanas, E. Membrane androgen receptor activation induces apoptotic regression of human prostate cancer cells in vitro and in vivo. *J. Clin. Endocrinol. Metab*. **2005**, *90*, 893–903.
(85) Wang, Z.; Liu, L.; Hou, J.; Wen, D.; Yan, C.; Pu, J.; Ouyang, J.; Pan, H. Rapid membrane effect of testosterone in LNCaP cells. *Urol. Int*. **2008**, *81*, 353–359.
(86) Dambaki, C.; Kogia, C.; Kampa, M.; Darivianaki, K.; Nomikos, M.; Anezinis, P.; Theodoropoulos, P. A.; Castanas, E.; Stathopoulos, E. N. Membrane testosterone binding sites in prostate carcinoma as a potential new marker and therapeutic target: study in paraffin tissue sections. *BMC Cancer* **2005**, *5*, 148.
(87) Makrigiorgos, G. M.; Berman, R. M.; Baranowska-Kortylewicz, J.; Bump, E.; Humm, J. L.; Adelstein, S. J.; Kassis, A. I. DNA damage produced in V79 cells by DNA-incorporated iodine-123: a comparison with iodine-125. *Radiat. Res*. **1992**, *129*, 309–314.
(88) Makrigiorgos, G. M.; Kassis, A. I.; Baranowska-Kortylewicz, J.; McElvany, K. D.; Welch, M. J.; Sastry, K. S.; Adelstein, S. J. Radiotoxicity of 5-[^{123}I]iodo-2′-deoxyuridine in V79 cells: a comparison with 5-[^{125}I]iodo-2′-deoxyuridine. *Radiat. Res*. **1989**, *118*, 532–544.
(89) Sharma, C. V.; Reddy, C. G.; Krishna, P. R. Zirconium(IV) chloride catalyzed new and efficient protocol for the selective cleavage of *p*-methoxybenzyl ethers. *J. Org. Chem*. **2003**, *68*, 4574–4575.
(90) Hoskins, J. M.; Meynell, G. G.; Sanders, F. K. A comparison of methods for estimating the viable count of a suspension of tumour cells. *Exp. Cell Res*. **1956**, *11*, 297–305.
(91) Heptinstall, J.; Rapley, R. Spectrophotometric Analysis of Nucleic Acids. In *The Nucleic Acid Protocols Handbook*; Rapley, R., Ed.; Humana Press: Totowa, NJ, 2000; pp 57−60.
(92) Skerrow, C. J.; Matoltsy, A. G. Isolation of epidermal desmosomes. *J. Cell Biol*. **1974**, *63*, 515–523.